Supporting Information for

Photophysical Properties of *N*-Methyl and *N*-Acetyl Substituted Alloxazine: A Theoretical Investigation

Huimin Guo†,[*], *Xiaolin Ma*†, *Zhiwen Lei*†, *Yang Qiu*†, *Jianzhang Zhao*†, *Bernhard Dick*‡

† State Key Laboratory of Fine Chemicals, Department of Chemistry, Dalian University of Technology, No. 2, Linggong Road, Dalian, 116024, P. R. China.

‡ Institut für Physikalische und Theoretische Chemie, Universität Regensburg, Universitätsstr. 31, Regensburg, 93053, Germany

KEYWORDS: Photophysics; Alloxazine; Intersystem Crossing; Internal Conversion; Absorption Spectrum; Emission Spectrum; Flavin.

[*] Corresponding authors, email: guohm@dlut.edu.cn (H. G.)

Theoretical Methods

Density Functional Theory (DFT) and Time-dependent Density Functional Theory (TD-DFT) based calculations were performed to investigate the photophysical properties of these compounds. Structures of the S_0 states of these compounds were fully optimized with the B3LYP functional with 6-311G(d) basis sets unless specified.[1-5] Benchmark calculations were also performed for Az and AAz1 at B3LYP/Def2TZVP level.[6, 7] TD-DFT calculations at the same level of theory were performed to get the fully relaxed S_1 and T_1 structures. All reported structures were verified with frequency calculations to be local minima on the corresponding potential energy surface. These calculations were performed with Gaussian 16.[8]

The transition dipole moments from T_1 to S_0 are evaluated from the quadratic response function[9-11] and the spin−orbit coupling matrix elements are computed at the same level of theory using the effective single-electron approximation in linear response theory with the Dalton program.[12-14]

The absorption, fluorescence and phosphorescence spectra of compounds, together with the radiative and non-radiative decay rate constants were calculated using MOMAP.[15-20] The absorption and fluorescence spectra were calculated according to eq-S1 and 2:

$$\sigma(\omega)_{abs} = \frac{4\pi^2\omega}{3\hbar c} \times \sum_{v_i,v_f} P_{iv_i}(T) \left|\left\langle \Theta_{f,v_f} \middle| \mu_{fi} \middle| \Theta_{i,v_i} \right\rangle\right|^2 \delta\left(\omega - \omega_{f,v_f,i,v_i}\right) \quad \text{(eq-S1)}$$

$$\sigma(\omega)_{emi} = \frac{4\omega^3}{3\hbar c} \times \sum_{v_i,v_f} P_{iv_i}(T) \left|\left\langle \Theta_{f,v_f} \middle| \mu_{fi} \middle| \Theta_{i,v_i} \right\rangle\right|^2 \delta\left(\omega_{i,v_i,f,v_f} - \omega\right) \quad \text{(eq-S2)}$$

where $P_{iv_i}(T)$ is the Boltzmann population of the vibrational manifolds in the initial state, $\mu_{fi} = \langle \Phi_f | \mu | \Phi_i \rangle$ is the electronic transition dipole moment between the initial state i and final state f calculated according to the Frank-Condon approximation, υ_i/υ_f is vibrational quantum number of state i/f, ω is the radiation frequency and $\omega_{i,\upsilon_i,f,\upsilon_f} = \omega_{f,\upsilon_f} - \omega_{i,\upsilon_i}$, respectively. The absorption and emission rate constants were calculated as the integration of the spectra.[20-23]

For the non-radiative decay, applying the second-order perturbation approximation, the rate constants were calculated as:

$$k_{f\leftarrow i} = \frac{2\pi}{\hbar}\sum_{\upsilon_i,\upsilon_f} P_{i\upsilon_i}\left|H'_{f\upsilon_f,i\upsilon_i} + \sum_{n,\upsilon_n}\frac{H'_{f\upsilon_f,n\upsilon_n}H'_{n\upsilon_n,i\upsilon_i}}{E_{i\upsilon_i}-E_{n\upsilon_n}}\right|^2 \times \delta\left(E_{i\upsilon_i} - E_{f\upsilon_f}\right) \quad \text{(eq-S3)}$$

where, υ_i/υ_f is vibrational quantum number of state i/f and H' is the interaction between 2 different Born-Oppenheimer states and calculated as $\mathrm{H}'\psi_{i\upsilon_i} = H^{NA}\Phi_i(r:Q)\Theta_{i\upsilon_i}(Q) + H^{SO}\Phi_i(r:Q)\Theta_{i\upsilon_i}(Q)$, where H^{NA} is the non-adiabatic coupling operator, H^{SO} is the spin-orbital coupling operator, r and Q are the electronic and nuclear normal mode coordinates.[24]

The transition dipole moment for phosphorescence was calculated as eq-S4:

$$\mu_{ST_\kappa} = \sum_k^{\{singlets\}}\frac{\langle S|\mu|\,{}^1k\rangle\langle\,{}^1k|H^{SO}|T_\kappa\rangle}{{}^3E_T^0 - {}^1E_k^0} + \sum_n^{\{triplets\}}\sum_{\kappa'=1}^{3}\frac{\langle S|H^{SO}|\,{}^3n_{\kappa'}\rangle\langle\,{}^3n_{\kappa'}|\mu|T_\kappa\rangle}{{}^1E_S^0 - {}^3E_n^0} \quad \text{(eq-S4)}$$

where κ is the magnetic quantum number, n and k are the intermediate triplet and singlet electronic states, respectively. Applying the Franck-Condon approximation, the phosphorescence spectra were calculated as eq-S5[19]:

$$\sigma_{ph}(\omega,T) = \frac{4\omega^3}{3\hbar c^3} \times \sum_{\upsilon_i,\upsilon_f} P_{i\upsilon_i}(T)\left|\left\langle\Theta_{f,\upsilon_f}\middle|\mu_{ST}\middle|\Theta_{i,\upsilon_i}\right\rangle\right|^2 \delta\left(\omega_{i,\upsilon_i,f,\upsilon_f} - \omega\right) \quad \text{(eq-S5)}$$

The radiative decay rate constant was calculated as the integration of the phosphorescence spectra.

The intersystem crossing rate constant can be calculated as:

$$k_{isc} = k_{isc}^{(0)} + k_{isc}^{(1)} + k_{isc}^{(2)} \quad \text{(eq-S6)}$$

where:

$$k_{isc}^{(0)} = \frac{2\pi}{\hbar}\sum_{\upsilon_i,\upsilon_f} P_{i\upsilon_i} \left|H'_{f\upsilon_f,i\upsilon_i}\right|^2 \times \delta\left(E_{i\upsilon_i} - E_{f\upsilon_f}\right) \quad \text{(eq-S7)}$$

$$k_{isc}^{(1)} = \frac{2\pi}{\hbar}\sum_{\upsilon_i,\upsilon_f} P_{i\upsilon_i} 2Re(H'_{f\upsilon_f,i\upsilon_i} \sum_{n,\upsilon_n} \frac{H'_{f\upsilon_f,n\upsilon_n} H'_{n\upsilon_n,i\upsilon_i}}{E_{i\upsilon_i} - E_{n\upsilon_n}}) \quad \times \delta\left(E_{i\upsilon_i} - E_{f\upsilon_f}\right) \quad \text{(eq-S8)}$$

$$k_{isc}^{(2)} = \frac{2\pi}{\hbar}\sum_{\upsilon_i,\upsilon_f} P_{i\upsilon_i} \left|\sum_{n,\upsilon_n} \frac{H'_{f\upsilon_f,n\upsilon_n} H'_{n\upsilon_n,i\upsilon_i}}{E_{i\upsilon_i} - E_{n\upsilon_n}}\right|^2 \times \delta\left(E_{i\upsilon_i} - E_{f\upsilon_f}\right) \text{(eq-S9)}$$

More details on calculation of these spectra and rate constants can be found in Ref. 15-24.

Natural Transition Orbital (NTO) analysis was performed to understand the electron transitions involved in absorption with Multiwfn and Gaussian 16.[8, 25] The polarizable continuum model (PCM) was applied to take into account the electrostatic interaction with the solvent.[26-28]

Table S1. Electronic transitions involved in the excitation of Az in visible light region.

No.	Energy	f[a]	Composition[b]	CI[c]	Character
$S_0 \to S_1$	3.4254 eV/361.96 nm	0.0842	55→56	0.69357	$\pi \to \pi^*$ $n \to \pi^*$
$S_0 \to S_2$	3.4586 eV/358.48 nm	0.0017	52→56	0.11814	$\pi \to \pi^*$
			53→56	0.69307	$n \to \pi^*$
$S_0 \to S_3$	3.9272 eV/315.70 nm	0.2381	54→56	0.67168	$\pi \to \pi^*$
			55→57	0.18574	$n \to \pi^*$
$S_0 \to S_4$	4.0849 eV/303.51 nm	0.0001	50→56	0.14401	$\pi \to \pi^*$
			52→56	0.67067	$n \to \pi^*$
			53→56	0.10483	
$S_0 \to S_5$	4.8262 eV/256.90 nm	0.0338	49→56	0.12590	$\pi \to \pi^*$
			51→56	0.64667	$n \to \pi^*$
			55→57	0.22269	
$S_0 \to S_6$	4.9392 eV/251.02 nm	0.0000	50→56	0.49943	$\pi \to \pi^*$
			52→56	0.12683	$n \to \pi^*$
			53→57	0.45775	
$S_0 \to S_7$	4.9990 eV/248.02 nm	0.0000	48→56	0.17662	$\pi \to \pi^*$
			50→56	0.45534	$n \to \pi^*$
			52→57	0.15259	
			53→57	0.47402	
$S_0 \to S_8$	5.0343 eV/246.28 nm	0.4939	49→56	0.37870	$\pi \to \pi^*$
			51→56	0.23143	$n \to \pi^*$
			54→56	0.11624	
			54→57	0.21190	
			55→57	0.47419	
$S_0 \to S_9$	5.1331 eV/241.54 nm	0.0000	48→56	0.66816	$\pi \to \pi^*$
			53→57	0.18788	$n \to \pi^*$
$S_0 \to S_{10}$	5.2824 eV/234.71 nm	0.2835	49→56	0.27255	$\pi \to \pi^*$
			51→56	0.13267	$n \to \pi^*$
			54→57	0.47179	
			55→57	0.37221	
			55→58	0.13761	
$S_0 \to S_{11}$	5.4229 eV/228.63 nm	0.4391	49→56	0.49042	$\pi \to \pi^*$
			54→56	0.12126	$n \to \pi^*$
			54→57	0.34128	
			55→57	0.17914	
			55→58	0.26725	
$S_0 \to S_{12}$	5.7341 eV/216.22 nm	0.0001	50→56	0.10283	$\pi \to \pi^*$
			52→57	0.66139	$n \to \pi^*$
			53→57	0.13585	
$S_0 \to S_{13}$	5.9634 eV/207.91 nm	0.1274	47→56	0.11716	$\pi \to \pi^*$
			54→57	0.25157	$n \to \pi^*$
			54→58	0.10061	
			54→59	0.17777	
			55→58	0.58308	
$S_0 \to S_{14}$	6.0553 eV/204.75 nm	0.0004	50→57	0.16242	$\pi \to \pi^*$
			52→57	0.10823	$n \to \pi^*$
			52→59	0.16149	
			53→58	0.62813	
			53→59	0.14678	
$S_0 \to S_{15}$	6.2259 eV/199.14 nm	0.0010	50→57	0.29150	$\pi \to \pi^*$
			52→58	0.32192	$n \to \pi^*$
			52→59	0.11116	
			53→58	0.23136	
			53→59	0.45758	
$S_0 \to S_{16}$	6.2289 eV/199.05 nm	0.1149	51→57	0.17187	$\pi \to \pi^*$
			55→59	0.64760	$n \to \pi^*$

$S_0 \rightarrow S_{17}$	6.3289 eV/195.90 nm	0.0146	47→56	0.11789	$\pi \rightarrow \pi^*$
			51→57	0.65773	$n \rightarrow \pi^*$
			54→58	0.10568	
			55→59	0.14091	
$S_0 \rightarrow S_{18}$	6.3513 eV/195.21 nm	0.2455	47→56	0.23526	$\pi \rightarrow \pi^*$
			49→57	0.19846	$n \rightarrow \pi^*$
			51→57	0.13639	
			54→58	0.55930	
			55→58	0.14735	
			55→59	0.14771	
			55→60	0.11166	
$S_0 \rightarrow S_{19}$	6.4828 eV/191.25 nm	0.0005	50→57	0.56095	$\pi \rightarrow \pi^*$
			53→59	0.37036	$n \rightarrow \pi^*$
$S_0 \rightarrow S_{20}$	6.6086 eV/187.61 nm	0.0009	46→56	0.67435	$\pi \rightarrow \pi^*$
			53→59	0.14710	$n \rightarrow \pi^*$
$S_0 \rightarrow T_1$	2.5212 eV/491.76 nm	0.0000	54→56	0.25642	$\pi \rightarrow \pi^*$
			54→58	0.10212	$n \rightarrow \pi^*$
			55→56	0.62402	
			55→57	0.14191	
$S_0 \rightarrow T_2$	2.8926 eV/428.63 nm	0.0000	54→56	0.62172	$\pi \rightarrow \pi^*$
			55→56	0.29624	$n \rightarrow \pi^*$
$S_0 \rightarrow T_3$	2.9682 eV/417.71 nm	0.0000	52→56	0.23021	$\pi \rightarrow \pi^*$
			53→56	0.64965	$n \rightarrow \pi^*$
$S_0 \rightarrow T_4$	3.7396 eV/331.54 nm	0.0000	48→56	0.10728	$\pi \rightarrow \pi^*$
			50→56	0.18638	$n \rightarrow \pi^*$
			52→56	0.59937	
			53→56	0.22494	
$S_0 \rightarrow T_5$	3.8940 eV/318.40 nm	0.0000	51→56	0.10904	$\pi \rightarrow \pi^*$
			54→56	0.16379	$n \rightarrow \pi^*$
			54→57	0.13378	
			55→56	0.10803	
			55→57	0.63844	

[a] Oscillator strength. It is zero for $S_0 \rightarrow T_n$ transitions.
[b] Only the main configurations are presented.
[c] The CI coefficients are in absolute values.

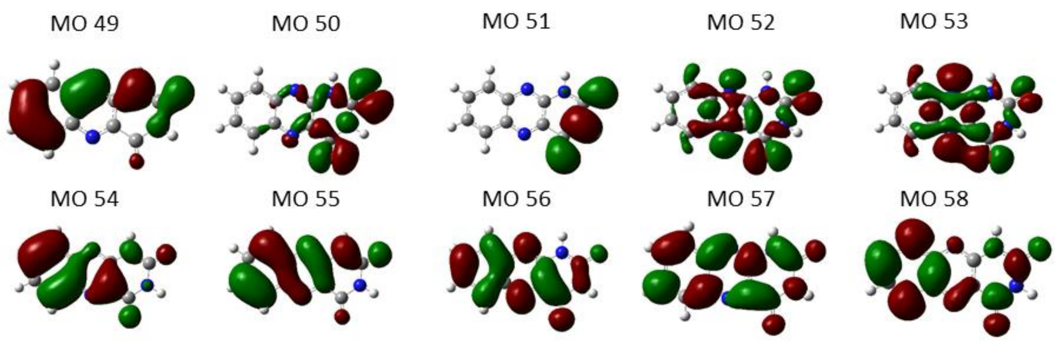

Figure S1. Contour plots of wavefunction of states of Az involved in absorption in visible light region. The C, O, N and H are in gray, red, blue and white, respectively. The isovalue is ±0.02 a.u.

Table S2. Electronic transitions involved in the excitation of AAz1 in visible light region.

No.	Energy	f[a]	Composition[b]	CI[c]	Character
$S_0 \to S_1$	3.4121 eV/363.36 nm	0.0707	64→67	0.12313	$\pi \to \pi^*$
			66→67	0.68101	$n \to \pi^*$
$S_0 \to S_2$	3.4405 eV/360.36 nm	0.0052	64→67	0.68184	$\pi \to \pi^*$
			66→67	0.13114	$n \to \pi^*$
$S_0 \to S_3$	3.9028 eV/317.68 nm	0.2356	65→67	0.66754	$\pi \to \pi^*$
			66→68	0.17660	$n \to \pi^*$
$S_0 \to S_4$	4.0630 eV/305.15 nm	0.0009	61→67	0.18013	$\pi \to \pi^*$
			63→67	0.65556	$n \to \pi^*$
$S_0 \to S_5$	4.6598 eV/266.07 nm	0.0027	61→69	0.16824	$\pi \to \pi^*$
			63→69	0.10531	$n \to \pi^*$
			65→69	0.15049	
			66→68	0.19022	
			66→69	0.61642	
$S_0 \to S_6$	4.7605 eV/260.44 nm	0.0288	61→67	0.38604	$\pi \to \pi^*$
			62→67	0.49011	$n \to \pi^*$
			63→67	0.16907	
			66→68	0.22632	
			66→69	0.10103	
$S_0 \to S_7$	4.8742 eV/254.37 nm	0.0186	60→67	0.22247	$\pi \to \pi^*$
			61→67	0.48502	$n \to \pi^*$
			62→67	0.36631	
			63→67	0.14575	
			64→68	0.11024	
			65→68	0.10348	
			66→68	0.14529	
$S_0 \to S_8$	4.9218 eV/251.91 nm	0.0041	58→67	0.16088	$\pi \to \pi^*$
			61→67	0.12510	$n \to \pi^*$
			64→68	0.64414	
$S_0 \to S_9$	5.0037 eV/247.78 nm	0.0470	59→69	0.16965	$\pi \to \pi^*$
			60→67	0.14756	$n \to \pi^*$
			61→69	0.32151	
			62→69	0.10951	
			63→69	0.30860	
			64→69	0.36317	
			66→68	0.17351	
			66→69	0.16571	
$S_0 \to S_{10}$	5.0131 eV/247.32 nm	0.3033	59→67	0.13792	$\pi \to \pi^*$
			60→67	0.38761	$n \to \pi^*$
			61→69	0.10549	
			62→67	0.26200	
			63→69	0.12308	
			64→69	0.12712	
			65→68	0.20444	
			66→68	0.32619	
			66→69	0.16571	
$S_0 \to S_{11}$	5.1036 eV/242.93 nm	0.1427	58→67	0.35711	$\pi \to \pi^*$
			59→67	0.31602	$n \to \pi^*$
			60→67	0.37793	
			64→68	0.16352	
			66→68	0.23387	
$S_0 \to S_{12}$	5.1551 eV/240.51 nm	0.1407	58→67	0.56107	$\pi \to \pi^*$
			59→67	0.11570	$n \to \pi^*$
			60→67	0.25042	
			61→67	0.14304	
			66→68	0.21933	

$S_0 \rightarrow S_{13}$	5.2513 eV/236.10 nm	0.1850	59→67	0.33719	$\pi \rightarrow \pi^*$
			62→67	0.12399	$n \rightarrow \pi^*$
			65→68	0.47193	
			66→68	0.26723	
			66→70	0.13629	
$S_0 \rightarrow S_{14}$	5.3946 eV/229.83 nm	0.2914	59→67	0.41935	$\pi \rightarrow \pi^*$
			60→67	0.17170	$n \rightarrow \pi^*$
			65→67	0.10072	
			65→68	0.33576	
			65→69	0.27067	
			66→68	0.15528	
			66→70	0.18144	
$S_0 \rightarrow S_{15}$	5.4348 eV/228.13 nm	0.0967	59→67	0.20590	$\pi \rightarrow \pi^*$
			64→69	0.21080	$n \rightarrow \pi^*$
			65→69	0.58517	
			66→69	0.12806	
			66→70	0.15009	
$S_0 \rightarrow S_{16}$	5.4883 eV/225.90 nm	0.0008	61→69	0.24678	$\pi \rightarrow \pi^*$
			63→68	0.11208	$n \rightarrow \pi^*$
			63→69	0.28860	
			64→69	0.51985	
			65→69	0.18363	
$S_0 \rightarrow S_{17}$	5.6833 eV/218.15 nm	0.0004	61→68	0.10578	$\pi \rightarrow \pi^*$
			63→68	0.64299	$n \rightarrow \pi^*$
			63→69	0.14145	
$S_0 \rightarrow S_{18}$	5.9370 eV/208.83 nm	0.0668	57→67	0.11613	$\pi \rightarrow \pi^*$
			65→68	0.20593	$n \rightarrow \pi^*$
			65→71	0.17004	
			66→70	0.59528	
			66→71	0.11436	
$S_0 \rightarrow S_{19}$	6.0319 eV/205.55 nm	0.0008	60→68	0.10416	$\pi \rightarrow \pi^*$
			60→69	0.11573	$n \rightarrow \pi^*$
			61→68	0.15245	
			61→69	0.13737	
			63→69	0.22399	
			63→71	0.15806	
			64→70	0.53247	
			64→71	0.12521	
$S_0 \rightarrow S_{20}$	6.0808 eV/203.90 nm	0.0006	59→69	0.15008	$\pi \rightarrow \pi^*$
			60→69	0.21026	$n \rightarrow \pi^*$
			61→69	0.29091	
			62→69	0.16412	
			63→68	0.10156	
			63→69	0.40550	
			64→70	0.32841	
$S_0 \rightarrow T_1$	2.5224 eV/491.54 nm	0.0000	65→67	0.27304	$\pi \rightarrow \pi^*$
			65→70	0.10117	$n \rightarrow \pi^*$
			66→67	0.61580	
			66→68	0.14080	
$S_0 \rightarrow T_2$	2.8848 eV/429.78 nm	0.0000	65→67	0.61495	$\pi \rightarrow \pi^*$
			66→67	0.31168	$n \rightarrow \pi^*$
$S_0 \rightarrow T_3$	2.9503 eV/420.24 nm	0.0000	61→67	0.11309	$\pi \rightarrow \pi^*$
			63→67	0.14144	$n \rightarrow \pi^*$
			64→67	0.66190	
$S_0 \rightarrow T_4$	3.7344 eV/332.00 nm	0.0000	60→67	0.13353	$\pi \rightarrow \pi^*$
			61→67	0.20967	$n \rightarrow \pi^*$
			63→67	0.58894	

			64→67	0.17594	
$S_0 \rightarrow T_5$	3.8813 eV/319.44 nm	0.0000	65→67	0.16064	$\pi \rightarrow \pi^*$
			65→68	0.13144	$n \rightarrow \pi^*$
			66→67	0.10996	
			66→68	0.62775	
			66→69	0.11992	

[a] Oscillator strength. It is zero for $S_0 \rightarrow T_n$ transitions.
[b] Only the main configurations are presented.
[c] The CI coefficients are in absolute values.

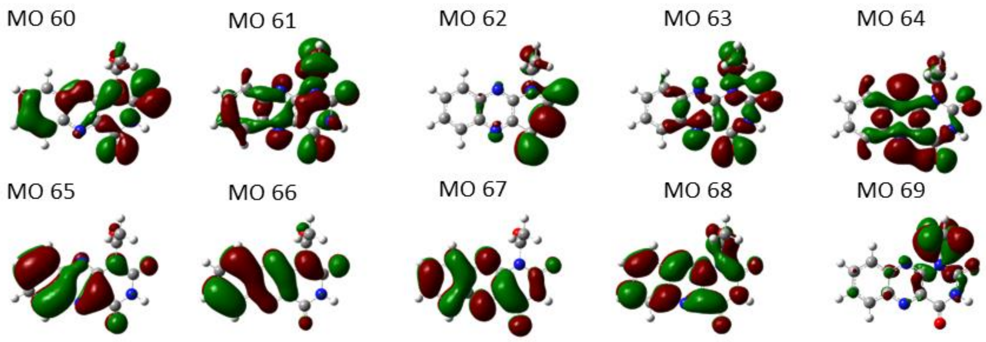

Figure S2. Contour plots of wavefunction of states of AAz1 involved in absorption in visible light region. The C, O, N and H are in gray, red, blue and white, respectively. The isovalue is ±0.02 a.u.

Table S3. Electronic transitions involved in the excitation of AAz3 in visible light region.

No.	Energy	f[a]	Composition[b]	CI[c]	Character
$S_0 \rightarrow S_1$	3.4004 eV/364.62 nm	0.0757	66→67	0.69374	$\pi \rightarrow \pi^*$ $n \rightarrow \pi^*$
$S_0 \rightarrow S_2$	3.4582 eV/358.53 nm	0.0017	64→67	0.69470	$\pi \rightarrow \pi^*$ $n \rightarrow \pi^*$
$S_0 \rightarrow S_3$	3.9005 eV/317.87 nm	0.2714	65→67	0.67110	$\pi \rightarrow \pi^*$
			66→68	0.18749	$n \rightarrow \pi^*$
$S_0 \rightarrow S_4$	4.1161 eV/301.21 nm	0.0002	59→67	0.12019	$\pi \rightarrow \pi^*$
			62→67	0.39330	$n \rightarrow \pi^*$
			63→67	0.54746	
$S_0 \rightarrow S_5$	4.5874 eV/270.27 nm	0.0027	62→67	0.56603	$\pi \rightarrow \pi^*$
			63→67	0.39676	$n \rightarrow \pi^*$
$S_0 \rightarrow S_6$	4.8330 eV/256.54 nm	0.0275	60→67	0.13346	$\pi \rightarrow \pi^*$
			61→67	0.63748	$n \rightarrow \pi^*$
			66→68	0.20103	
$S_0 \rightarrow S_7$	4.9671 eV/249.61 nm	0.0035	58→67	0.12272	$\pi \rightarrow \pi^*$
			61→69	0.11932	$n \rightarrow \pi^*$
			62→69	0.19438	
			63→69	0.26507	
			64→68	0.56219	
$S_0 \rightarrow S_8$	4.9759 eV/249.17 nm	0.0006	59→69	0.11810	$\pi \rightarrow \pi^*$
			61→69	0.17791	$n \rightarrow \pi^*$
			62→69	0.29849	
			63→68	0.10354	
			63→69	0.37366	
			64→68	0.35155	
			64→69	0.21709	
			66→69	0.15681	
$S_0 \rightarrow S_9$	5.0166 eV/247.15 nm	0.5879	59→67	0.11838	$\pi \rightarrow \pi^*$
			60→67	0.32258	$n \rightarrow \pi^*$
			61→67	0.20719	
			65→67	0.12432	
			65→68	0.19814	
			66→68	0.49692	
$S_0 \rightarrow S_{10}$	5.0769 eV/244.21 nm	0.0074	63→69	0.10556	$\pi \rightarrow \pi^*$
			65→69	0.13860	$n \rightarrow \pi^*$
			66→69	0.65807	
$S_0 \rightarrow S_{11}$	5.1015 eV/243.03 nm	0.0000	58→67	0.53569	$\pi \rightarrow \pi^*$
			59→67	0.39739	$n \rightarrow \pi^*$
			60→67	0.12263	
			64→68	0.12726	
$S_0 \rightarrow S_{12}$	5.2307 eV/237.03 nm	0.1436	58→67	0.29277	$\pi \rightarrow \pi^*$
			59→67	0.27799	$n \rightarrow \pi^*$
			60→67	0.31028	
			65→68	0.34323	
			66→68	0.25993	
$S_0 \rightarrow S_{13}$	5.2830 eV/234.69 nm	0.1251	58→67	0.27853	$\pi \rightarrow \pi^*$
			59→67	0.42069	$n \rightarrow \pi^*$
			61→67	0.15097	
			65→68	0.34787	
			66→68	0.22796	
			66→70	0.10610	
$S_0 \rightarrow S_{14}$	5.3946 eV/229.83 nm	0.4372	59→67	0.17439	$\pi \rightarrow \pi^*$
			60→67	0.48171	$n \rightarrow \pi^*$
			65→67	0.11788	
			65→68	0.33290	
			66→68	0.17194	
			66→70	0.22741	

$S_0 \rightarrow S_{15}$	5.5177 eV/224.70 nm	0.0045	62→69	0.36229	$\pi \rightarrow \pi^*$
			64→69	0.58650	$n \rightarrow \pi^*$
			65→69	0.12073	
$S_0 \rightarrow S_{16}$	5.5745 eV/222.41 nm	0.0002	61→69	0.10343	$\pi \rightarrow \pi^*$
			65→69	0.67257	$n \rightarrow \pi^*$
			66→69	0.13238	
$S_0 \rightarrow S_{17}$	5.7711 eV/214.84 nm	0.0001	59→67	0.12089	$\pi \rightarrow \pi^*$
			62→68	0.38090	$n \rightarrow \pi^*$
			63→68	0.52789	
			64→68	0.11619	
$S_0 \rightarrow S_{18}$	5.8211 eV/212.99 nm	0.0000	61→69	0.63158	$\pi \rightarrow \pi^*$
			62→69	0.14690	$n \rightarrow \pi^*$
			63→69	0.20297	
$S_0 \rightarrow S_{19}$	5.9384 eV/208.78 nm	0.0771	57→67	0.12016	$\pi \rightarrow \pi^*$
			65→68	0.21615	$n \rightarrow \pi^*$
			65→71	0.18167	
			66→70	0.59756	
			66→71	0.10135	
$S_0 \rightarrow S_{20}$	6.0383 eV/205.33 nm	0.0005	59→68	0.10498	$\pi \rightarrow \pi^*$
			61→68	0.12682	$n \rightarrow \pi^*$
			62→68	0.45949	
			62→69	0.16562	
			63→68	0.26595	
			63→69	0.10931	
			64→70	0.31592	
$S_0 \rightarrow T_1$	2.5038 eV/495.18 nm	0.0000	65→67	0.25026	$\pi \rightarrow \pi^*$
			66→67	0.62592	$n \rightarrow \pi^*$
			66→68	0.14226	
$S_0 \rightarrow T_2$	2.8832 eV/430.02 nm	0.0000	65→67	0.62606	$\pi \rightarrow \pi^*$
			66→67	0.28950	$n \rightarrow \pi^*$
$S_0 \rightarrow T_3$	2.9622 eV/418.55 nm	0.0000	62→67	0.11267	$\pi \rightarrow \pi^*$
			63→67	0.17322	$n \rightarrow \pi^*$
			64→67	0.65688	
$S_0 \rightarrow T_4$	3.7745 eV/328.47 nm	0.0000	59→67	0.16890	$\pi \rightarrow \pi^*$
			62→67	0.36651	$n \rightarrow \pi^*$
			63→67	0.48851	
			64→67	0.20573	
$S_0 \rightarrow T_5$	3.8782 eV/319.69 nm	0.0000	65→67	0.15933	$\pi \rightarrow \pi^*$
			65→68	0.14437	$n \rightarrow \pi^*$
			66→67	0.11309	
			66→68	0.63066	

[a] Oscillator strength. It is zero for $S_0 \rightarrow T_n$ transitions.
[b] Only the main configurations are presented.
[c] The CI coefficients are in absolute values.

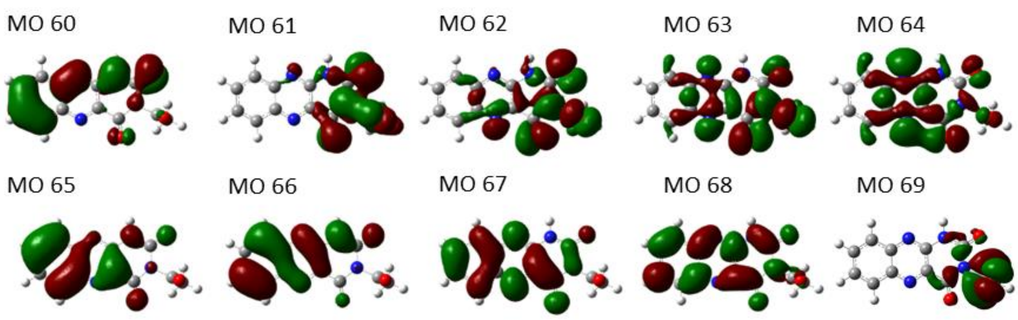

Figure S3. Contour plots of wavefunction of states of AAz3 involved in absorption in visible light region. The C, O, N and H are in gray, red, blue and white, respectively. The isovalue is ±0.02 a.u.

Table S4. Electronic transitions involved in the excitation of AAz13 in visible light region.

No.	**Energy**	**f[a]**	**Composition[b]**	**CI[c]**	**Character**
$S_0 \rightarrow S_1$	3.3870 eV/366.06 nm	0.0671	77→78	0.69303	$\pi\rightarrow\pi^*$ $n\rightarrow\pi^*$
$S_0 \rightarrow S_2$	3.4297 eV/361.51 nm	0.0017	75→78	0.69291	$\pi\rightarrow\pi^*$ $n\rightarrow\pi^*$
$S_0 \rightarrow S_3$	3.8779 eV/319.72 nm	0.2657	76→78	0.66946	$\pi\rightarrow\pi^*$
			77→79	0.14645	$n\rightarrow\pi^*$
			77→80	0.10979	
$S_0 \rightarrow S_4$	4.0997 eV/302.42 nm	0.0007	71→78	0.10672	$\pi\rightarrow\pi^*$
			72→78	0.11810	$n\rightarrow\pi^*$
			73→78	0.30039	
			74→78	0.59091	
$S_0 \rightarrow S_5$	4.5228 eV/274.13 nm	0.0010	73→78	0.59607	$\pi\rightarrow\pi^*$
			74→78	0.33949	$n\rightarrow\pi^*$
$S_0 \rightarrow S_6$	4.6300 eV/267.78 nm	0.0007	76→80	0.11415	$\pi\rightarrow\pi^*$
			77→79	0.39166	$n\rightarrow\pi^*$
			77→80	0.47005	
			77→81	0.21968	
$S_0 \rightarrow S_7$	4.8231 eV/257.06 nm	0.0446	70→78	0.14029	$\pi\rightarrow\pi^*$
			71→78	0.12206	$n\rightarrow\pi^*$
			72→78	0.60165	
			77→79	0.17993	
			77→80	0.17290	
$S_0 \rightarrow S_8$	4.8965 eV/253.21 nm	0.0764	68→78	0.17052	$\pi\rightarrow\pi^*$
			71→78	0.51095	$n\rightarrow\pi^*$
			72→78	0.20063	
			73→78	0.13509	
			75→79	0.25348	
			77→79	0.13108	
			77→80	0.15499	
$S_0 \rightarrow S_9$	4.9183 eV/252.09 nm	0.0682	71→78	0.21466	$\pi\rightarrow\pi^*$
			75→79	0.52324	$n\rightarrow\pi^*$
			75→80	0.27912	
			76→79	0.10717	
			77→79	0.17658	
$S_0 \rightarrow S_{10}$	4.9363 eV/251.17 nm	0.0003	71→81	0.20422	$\pi\rightarrow\pi^*$
			73→79	0.19743	$n\rightarrow\pi^*$
			73→80	0.25317	
			73→81	0.26928	
			74→79	0.12064	
			74→80	0.16399	
			75→79	0.11110	
			75→80	0.39196	
			77→80	0.10751	
$S_0 \rightarrow S_{11}$	4.9981 eV/248.06 nm	0.0014	71→79	0.18106	$\pi\rightarrow\pi^*$
			71→80	0.23038	$n\rightarrow\pi^*$
			72→81	0.11828	
			73→79	0.12648	
			73→80	0.19936	
			73→81	0.27859	
			74→79	0.10364	
			74→80	0.13019	
			74→81	0.18865	
			75→80	0.14587	
			75→81	0.27062	
			77→80	0.17423	

$S_0 \rightarrow S_{12}$	5.0385 eV/246.07 nm	0.4347	68→78	0.24664	$\pi \rightarrow \pi^*$
			70→78	0.31953	$n \rightarrow \pi^*$
			71→78	0.26490	
			72→78	0.19536	
			75→79	0.11688	
			76→79	0.11291	
			77→79	0.31606	
			77→80	0.23284	
$S_0 \rightarrow S_{13}$	5.1480 eV/240.84 nm	0.0921	68→78	0.36516	$\pi \rightarrow \pi^*$
			69→78	0.17962	$n \rightarrow \pi^*$
			70→78	0.10509	
			71→78	0.18330	
			76→80	0.12016	
			77→80	0.22550	
			77→81	0.42386	
$S_0 \rightarrow S_{14}$	5.1595 eV/240.30 nm	0.0845	68→78	0.35968	$\pi \rightarrow \pi^*$
			69→78	0.16994	$n \rightarrow \pi^*$
			71→78	0.18790	
			77→79	0.20088	
			77→81	0.46414	
$S_0 \rightarrow S_{15}$	5.2034 eV/238.28 nm	0.1215	68→78	0.29187	$\pi \rightarrow \pi^*$
			70→78	0.32097	$n \rightarrow \pi^*$
			76→79	0.37849	
			76→80	0.22463	
			77→79	0.18602	
			77→80	0.14033	
			77→82	0.10729	
$S_0 \rightarrow S_{16}$	5.2890 eV/234.42 nm	0.0361	68→78	0.18665	$\pi \rightarrow \pi^*$
			69→78	0.56549	$n \rightarrow \pi^*$
			70→78	0.10726	
			72→78	0.14221	
			76→79	0.21579	
			76→80	0.10063	
$S_0 \rightarrow S_{17}$	5.3252 eV/232.83 nm	0.0167	70→78	0.12236	$\pi \rightarrow \pi^*$
			76→79	0.41037	$n \rightarrow \pi^*$
			76→80	0.49553	
			77→79	0.11319	
$S_0 \rightarrow S_{18}$	5.3808 eV/230.42 nm	0.3565	69→78	0.23612	$\pi \rightarrow \pi^*$
			70→78	0.45006	$n \rightarrow \pi^*$
			76→78	0.10740	
			76→79	0.16303	
			76→80	0.31424	
			77→79	0.10075	
			77→80	0.11134	
			77→82	0.19438	
			77→83	0.10321	
$S_0 \rightarrow S_{19}$	5.4120 eV/229.09 nm	0.0059	71→81	0.13047	$\pi \rightarrow \pi^*$
			73→80	0.13730	$n \rightarrow \pi^*$
			74→79	0.24723	
			74→80	0.30936	
			75→79	0.28368	
			75→80	0.41320	
$S_0 \rightarrow S_{20}$	5.6650 eV/218.86 nm	0.0000	72→80	0.11828	$\pi \rightarrow \pi^*$
			74→81	0.17499	$n \rightarrow \pi^*$
			75→81	0.26956	
			76→81	0.58030	
$S_0 \rightarrow T_1$	2.5039 eV/495.16 nm	0.0000	76→78	0.26468	$\pi \rightarrow \pi^*$

			77→78	0.61925	n→π*
			77→79	0.11855	
S_0→T_2	2.8743 eV/431.36 nm	0.0000	76→78	0.62039	π→π*
			77→78	0.30270	n→π*
S_0→T_3	2.9390 eV/421.86 nm	0.0000	73→78	0.13105	π→π*
			75→78	0.66190	n→π*
S_0→T_4	3.7694 eV/328.93 nm	0.0000	69→78	0.13202	π→π*
			71→78	0.12464	n→π*
			72→78	0.12421	
			73→78	0.27941	
			74→78	0.53616	
			75→78	0.16110	
S_0→T_5	3.8661 Ev/320.70 nm	0.0000	76→78	0.15679	π→π*
			76→79	0.11613	n→π*
			77→78	0.11426	
			77→79	0.51521	
			77→80	0.36897	

[a] Oscillator strength. It is zero for S_0→T_n transitions.
[b] Only the main configurations are presented.
[c] The CI coefficients are in absolute values.

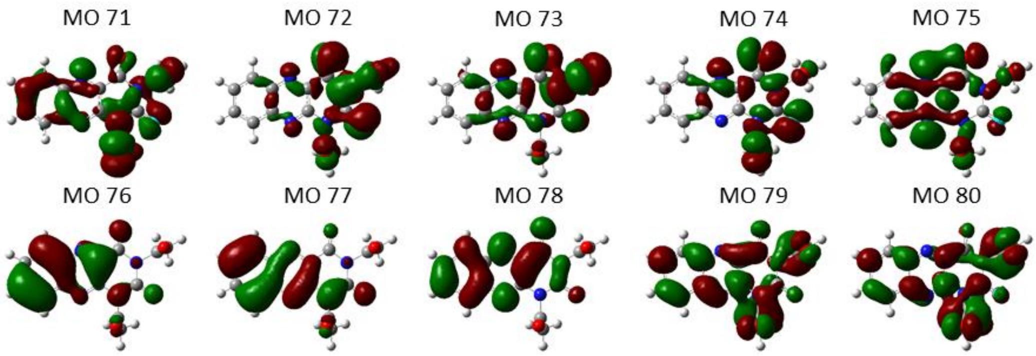

Figure S4. Contour plots of wavefunction of states of AAz13 involved in absorption in visible light region. The C, O, N and H are in gray, red, blue and white, respectively. The isovalue is ±0.02 a.u.

Table S5. Electronic transitions involved in the excitation of AAz13-1 in visible light region.

No.	Energy	f[a]	Composition[b]	CI[c]	Character
S_0→S_1	3.3872 eV/366.04 nm	0.0637	75 → 78	0.11370	π→π*
			77 → 78	0.68306	n→π*
S_0→S_2	3.4305 eV/361.41 nm	0.0049	75 → 78	0.68130	π→π*
			77 → 78	0.12338	n→π*
S_0→S_3	3.8793 eV/319.61 nm	0.2656	76 → 78	0.66628	π→π*
			77 → 79	0.15131	n→π*
			77 → 80	0.10369	
S_0→S_4	4.1014 eV/302.30 nm	0.0003	69 → 78	0.10330	π→π*
			72 → 78	0.18826	n→π*
			74 → 78	0.64825	
S_0→S_5	4.5703 eV/271.28 nm	0.0018	72 → 78	0.10046	π→π*
			73 → 78	0.67996	n→π*
			74 → 78	0.10245	
S_0→S_6	4.6330 eV/267.61 nm	0.0046	76 → 80	0.12063	π→π*
			77 → 79	0.40719	n→π*
			77 → 80	0.45163	
			77 → 81	0.22058	
S_0→S_7	4.7147 eV/262.97 nm	0.0176	71 → 78	0.13530	π→π*
			72 → 78	0.60038	n→π*

			74 → 78	0.19323	
			77 → 79	0.14701	
			77 → 80	0.18471	
$S_0 \rightarrow S_8$	4.8993 eV/253.07 nm	0.0037	68 → 78	0.13766	$\pi \rightarrow \pi^*$
			73 → 80	0.12536	$n \rightarrow \pi^*$
			75 → 79	0.59402	
			75 → 80	0.16856	
$S_0 \rightarrow S_9$	4.9341 eV/251.28 nm	0.0070	71 → 78	0.11262	$\pi \rightarrow \pi^*$
			71 → 81	0.15031	$n \rightarrow \pi^*$
			72 → 79	0.11554	
			72 → 80	0.11226	
			73 → 79	0.18242	
			73 → 80	0.25640	
			73 → 81	0.25246	
			74 → 81	0.13847	
			75 → 80	0.41578	
			77 → 80	0.15850	
$S_0 \rightarrow S_{10}$	4.9781 eV/249.06 nm	0.1207	68 → 78	0.14793	$\pi \rightarrow \pi^*$
			71 → 78	0.55584	$n \rightarrow \pi^*$
			72 → 78	0.21250	
			76 → 79	0.20425	
			76 → 80	0.12377	
			77 → 79	0.14104	
			77 → 80	0.12234	
$S_0 \rightarrow S_{11}$	5.0108 eV/247.44 nm	0.1770	70 → 78	0.17107	$\pi \rightarrow \pi^*$
			71 → 78	0.11250	$n \rightarrow \pi^*$
			71 → 79	0.11926	
			71 → 80	0.15595	
			72 → 81	0.13727	
			73 → 80	0.16351	
			73 → 81	0.23577	
			74 → 79	0.12904	
			74 → 80	0.18164	
			75 → 80	0.19710	
			75 → 81	0.23668	
			77 → 79	0.28885	
$S_0 \rightarrow S_{12}$	5.0233 eV/246.82 nm	0.3383	68 → 78	0.18465	$\pi \rightarrow \pi^*$
			70 → 78	0.27732	$n \rightarrow \pi^*$
			71 → 78	0.14126	
			73 → 80	0.13934	
			73 → 81	0.21011	
			74 → 80	0.10036	
			75 → 79	0.12016	
			75 → 81	0.14862	
			77 → 79	0.25033	
			77 → 80	0.29919	
$S_0 \rightarrow S_{13}$	5.1348 eV/41.46 nm	0.0272	68 → 78	0.24458	$\pi \rightarrow \pi^*$
			76 → 80	0.12515	$n \rightarrow \pi^*$
			76 → 81	0.10097	
			77 → 80	0.25045	
			77 → 81	0.54908	
$S_0 \rightarrow S_{14}$	5.1518 eV/240.66 nm	0.1380	68 → 78	0.48239	$\pi \rightarrow \pi^*$
			69 → 78	0.17365	$n \rightarrow \pi^*$
			71 → 78	0.19625	
			77 → 79	0.20262	
			77 → 81	0.32070	
$S_0 \rightarrow S_{15}$	5.2344 eV/236.87 nm	0.0960	68 → 78	0.11202	$\pi \rightarrow \pi^*$

			69 → 78	0.29226	n→π*
			70 → 78	0.25360	
			71 → 78	0.16708	
			76 → 79	0.42666	
			76 → 80	0.18359	
			77 → 79	0.14415	
			77 → 80	0.11234	
			77 → 82	0.13050	
S_0→S_{16}	5.2799 eV/234.82 nm	0.0310	68 → 78	0.27052	π→π*
			69 → 78	0.56447	n→π*
			72 → 78	0.11608	
			74 → 79	0.10942	
			76 → 79	0.14591	
S_0→S_{17}	5.3283 eV/232.69 nm	0.0284	70 → 78	0.18859	π→π*
			75 → 79	0.11249	n→π*
			75 → 80	0.16006	
			76 → 79	0.35783	
			76 → 80	0.50497	
			77 → 79	0.12590	
S_0→S_{18}	5.3861 eV/230.19 nm	0.3461	70 → 78	0.49111	π→π*
			71 → 78	0.13715	n→π*
			76 → 78	0.10577	
			76 → 79	0.15266	
			76 → 80	0.31671	
			77 → 80	0.11891	
			77 → 82	0.18997	
			77 → 83	0.10150	
S_0→S_{19}	5.4245 eV/228.56 nm	0.0019	71 → 81	0.10127	π→π*
			72 → 80	0.10588	n→π*
			72 → 81	0.10133	
			73 → 79	0.13553	
			73 → 80	0.21607	
			74 → 79	0.20497	
			74 → 80	0.25694	
			75 → 79	0.25520	
			75 → 80	0.41353	
			76 → 80	0.10484	
S_0→S_{20}	5.6449 eV/219.64 nm	0.0003	72 → 79	0.10708	π→π*
			72 → 80	0.20538	n→π*
			73 → 81	0.16570	
			74 → 81	0.19956	
			75 → 81	0.52164	
			76 → 81	0.23823	
S_0→T_1	2.5038 eV/495.18 nm	0	76 → 78	0.26500	π→π*
			77 → 78	0.61888	n→π*
			77 → 79	0.11959	
S_0→T_2	2.8766 eV/431.01 nm	0	76 → 78	0.61996	π→π*
			77 → 78	0.30317	n→π*
S_0→T_3	2.9391 eV/421.85 nm	0	72 → 78	0.10570	π→π*
			74 → 78	0.11111	n→π*
			75 → 78	0.66314	
S_0→T_4	3.7719 eV/328.70 nm	0	69 → 78	0.14644	π→π*
			72 → 78	0.19673	n→π*
			74 → 78	0.58814	
			75 → 78	0.15896	
S_0→T_5	3.8653 eV/320.76 nm	0	76 → 78	0.15593	π→π*
			76 → 79	0.12096	n→π*

77 → 78	0.11488
77 → 79	0.53040
77 → 80	0.34553

[a] Oscillator strength. It is zero for $S_0 \rightarrow T_n$ transitions.
[b] Only the main configurations are presented.
[c] The CI coefficients are in absolute values.

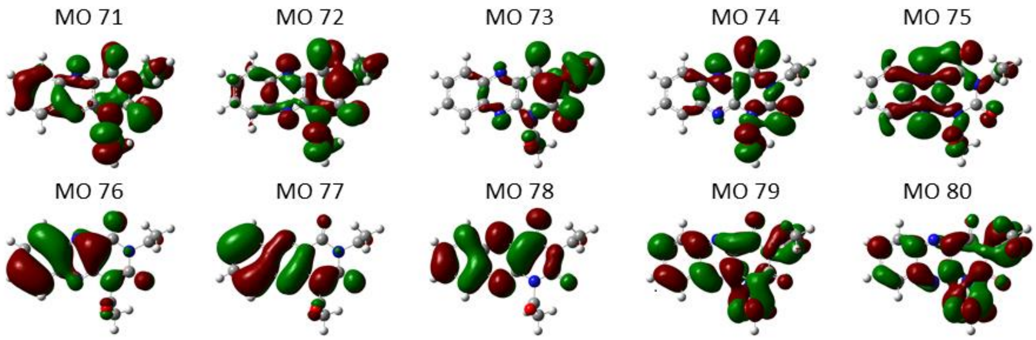

Figure S5. Contour plots of wavefunction of states of AAz13-1 involved in absorption in visible light region. The C, O, N and H are in gray, red, blue and white, respectively. The isovalue is ±0.02 a.u.

Table S6. Electronic transitions involved in the excitation of AzMe in visible light region.

No.	Energy	f[a]	Composition[b]	CI[c]	Character
$S_0 \rightarrow S_1$	3.3868 eV/366.08 nm	0.1004	59→60	0.69417	$\pi \rightarrow \pi^*$ $n \rightarrow \pi^*$
$S_0 \rightarrow S_2$	3.4382 eV/360.61 nm	0.0015	56→60	0.11117	$\pi \rightarrow \pi^*$
			57→60	0.69423	$n \rightarrow \pi^*$
$S_0 \rightarrow S_3$	3.9073 eV/317.32 nm	0.2054	58→60	0.67530	$\pi \rightarrow \pi^*$
			59→61	0.17158	$n \rightarrow \pi^*$
$S_0 \rightarrow S_4$	4.0627 eV/305.18 nm	0.0001	53→60	0.13877	$\pi \rightarrow \pi^*$
			56→60	0.67234	$n \rightarrow \pi^*$
$S_0 \rightarrow S_5$	4.7424 eV/261.44 nm	0.0704	54→60	0.24276	$\pi \rightarrow \pi^*$
			55→60	0.54867	$n \rightarrow \pi^*$
			59→61	0.35192	
$S_0 \rightarrow S_6$	4.8916 eV/253.46 nm	0.0000	52→60	0.19142	$\pi \rightarrow \pi^*$
			53→60	0.35272	$n \rightarrow \pi^*$
			57→61	0.55978	
$S_0 \rightarrow S_7$	4.9590 eV/250.02 nm	0.1523	54→60	0.45982	$\pi \rightarrow \pi^*$
			55→60	0.37754	$n \rightarrow \pi^*$
			58→61	0.27367	
			59→61	0.23625	
$S_0 \rightarrow S_8$	4.9767 eV/249.13 nm	0.0000	53→60	0.57259	$\pi \rightarrow \pi^*$
			56→60	0.10278	$n \rightarrow \pi^*$
			56→61	0.14821	
			57→61	0.36168	
$S_0 \rightarrow S_9$	5.0724 eV/244.43 nm	0.0001	52→60	0.67056	$\pi \rightarrow \pi^*$
			57→61	0.16425	$n \rightarrow \pi^*$
$S_0 \rightarrow S_{10}$	5.1193 eV/242.19 nm	0.6284	54→60	0.26438	$\pi \rightarrow \pi^*$
			55→60	0.21831	$n \rightarrow \pi^*$
			58→60	0.11573	
			58→61	0.29633	
			59→61	0.50927	
$S_0 \rightarrow S_{11}$	5.3655 eV/231.08 nm	0.4300	54→60	0.36793	$\pi \rightarrow \pi^*$
			58→60	0.10478	$n \rightarrow \pi^*$
			58→61	0.46594	
			59→61	0.11363	
			59→62	0.31299	
$S_0 \rightarrow S_{12}$	5.6979 eV/217.60 nm	0.0000	53→60	0.10717	$\pi \rightarrow \pi^*$
			56→61	0.66590	$n \rightarrow \pi^*$
			57→61	0.13502	
$S_0 \rightarrow S_{13}$	5.8932 eV/210.38 nm	0.1230	51→60	0.10952	$\pi \rightarrow \pi^*$
			58→61	0.27458	$n \rightarrow \pi^*$
			58→63	0.14819	
			59→62	0.58908	
$S_0 \rightarrow S_{14}$	6.0177 eV/206.03 nm	0.0006	53→61	0.12372	$\pi \rightarrow \pi^*$
			56→63	0.14350	$n \rightarrow \pi^*$
			57→62	0.65735	
$S_0 \rightarrow S_{15}$	6.1950 eV/200.14 nm	0.1126	55→61	0.22107	$\pi \rightarrow \pi^*$
			59→63	0.64438	$n \rightarrow \pi^*$
$S_0 \rightarrow S_{16}$	6.2057 eV/199.79 nm	0.0007	53→61	0.32994	$\pi \rightarrow \pi^*$
			53→64	0.10126	$n \rightarrow \pi^*$
			56→62	0.32400	
			56→63	0.13850	
			57→62	0.15085	
			57→63	0.45632	
$S_0 \rightarrow S_{17}$	6.2769 eV/197.52 nm	0.0709	51→60	0.20245	$\pi \rightarrow \pi^*$
			54→61	0.15494	$n \rightarrow \pi^*$
			55→61	0.50891	
			58→62	0.36337	

			59→63	0.10564	
$S_0 \rightarrow S_{18}$	6.3198 eV/196.18 nm	0.1340	51→60	0.12058	$\pi\rightarrow\pi^*$
			54→61	0.25076	$n\rightarrow\pi^*$
			55→61	0.41820	
			58→62	0.42869	
			59→63	0.19610	
$S_0 \rightarrow S_{19}$	6.4690 eV/191.66 nm	0.0006	53→61	0.55065	$\pi\rightarrow\pi^*$
			57→63	0.40084	$n\rightarrow\pi^*$
$S_0 \rightarrow S_{20}$	6.5716 eV/188.67 nm	0.0003	52→61	0.68581	$\pi\rightarrow\pi^*$ $n\rightarrow\pi^*$
$S_0 \rightarrow T_1$	2.5365 eV/488.80 nm	0.0000	58→60	0.27880	$\pi\rightarrow\pi^*$
			58→62	0.10742	$n\rightarrow\pi^*$
			59→60	0.61543	
			59→61	0.14077	
$S_0 \rightarrow T_2$	2.8600 eV/433.51 nm	0.0000	58→60	0.60579	$\pi\rightarrow\pi^*$
			59→60	0.31870	$n\rightarrow\pi^*$
$S_0 \rightarrow T_3$	2.9572 eV/419.26 nm	0.0000	56→60	0.21859	$\pi\rightarrow\pi^*$
			57→60	0.65342	$n\rightarrow\pi^*$
$S_0 \rightarrow T_4$	3.7196 eV/333.33 nm	0.0000	52→60	0.12415	$\pi\rightarrow\pi^*$
			53→60	0.17458	$n\rightarrow\pi^*$
			56→60	0.60473	
			57→60	0.21623	
$S_0 \rightarrow T_5$	3.8641 eV/320.86 nm	0.0000	55→60	0.10225	$\pi\rightarrow\pi^*$
			58→60	0.17798	$n\rightarrow\pi^*$
			59→61	0.64565	

[a] Oscillator strength. It is zero for $S_0 \rightarrow T_n$ transitions.
[b] Only the main configurations are presented.
[c] The CI coefficients are in absolute values.

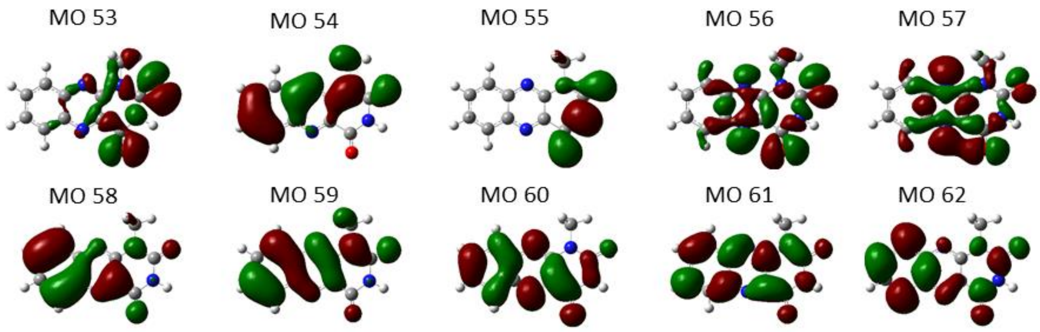

Figure S6. Contour plots of wavefunction of states of AzMe involved in absorption in visible light region. The C, O, N and H are in gray, red, blue and white, respectively. The isovalue is ±0.02 a.u.

Table S7. Electronic transitions involved in the excitation of AAz3Me in visible light region.

No.	Energy	f[a]	Composition[b]	CI[c]	Character
$S_0 \rightarrow S_1$	3.3668 eV/368.25 nm	0.0919	70→71	0.69392	$\pi \rightarrow \pi^*$ $n \rightarrow \pi^*$
$S_0 \rightarrow S_2$	3.4335 eV/361.10 nm	0.0016	68→71	0.69520	$\pi \rightarrow \pi^*$ $n \rightarrow \pi^*$
$S_0 \rightarrow S_3$	3.8788 eV/319.65 nm	0.2361	69→71	0.67460	$\pi \rightarrow \pi^*$
			70→72	0.17300	$n \rightarrow \pi^*$
$S_0 \rightarrow S_4$	4.0908 eV/303.08 nm	0.0001	63→71	0.12036	$\pi \rightarrow \pi^*$
			66→71	0.21108	$n \rightarrow \pi^*$
			67→71	0.64150	
$S_0 \rightarrow S_5$	4.5716 eV/271.20 nm	0.0018	66→71	0.64236	$\pi \rightarrow \pi^*$
			67→71	0.20684	$n \rightarrow \pi^*$
			70→72	0.16099	
$S_0 \rightarrow S_6$	4.7727 eV/259.78 nm	0.0747	62→71	0.10102	$\pi \rightarrow \pi^*$
			64→71	0.20678	$n \rightarrow \pi^*$
			65→71	0.56739	
			68→72	0.10002	
			70→72	0.29950	
$S_0 \rightarrow S_7$	4.9087 eV/252.58 nm	0.0214	62→71	0.15986	$\pi \rightarrow \pi^*$
			67→72	0.11510	$n \rightarrow \pi^*$
			68→72	0.64819	
			70→72	0.10524	
$S_0 \rightarrow S_8$	4.9530 eV/250.32 nm	0.2068	64→71	0.41542	$\pi \rightarrow \pi^*$
			65→71	0.33878	$n \rightarrow \pi^*$
			66→71	0.12030	
			68→72	0.11661	
			69→72	0.25559	
			70→72	0.27084	
			70→73	0.10097	
$S_0 \rightarrow S_9$	4.9639 eV/249.77 nm	0.0046	63→73	0.11573	$\pi \rightarrow \pi^*$
			65→73	0.17337	$n \rightarrow \pi^*$
			66→73	0.35211	
			67→73	0.24401	
			68→73	0.19393	
			70→73	0.45984	
$S_0 \rightarrow S_{10}$	5.0184 eV/247.06 nm	0.0251	63→73	0.10688	$\pi \rightarrow \pi^*$
			64→71	0.10602	$n \rightarrow \pi^*$
			65→73	0.18040	
			66→73	0.28614	
			67→73	0.21127	
			68→73	0.18698	
			69→72	0.10647	
			69→73	0.11953	
			70→72	0.12415	
			70→73	0.48071	
$S_0 \rightarrow S_{11}$	5.0682 eV/244.63 nm	0.0093	62→71	0.64707	$\pi \rightarrow \pi^*$
			63→71	0.15994	$n \rightarrow \pi^*$
			68→72	0.15559	
$S_0 \rightarrow S_{12}$	5.0916 eV/243.51 nm	0.5402	63→71	0.15239	$\pi \rightarrow \pi^*$
			64→71	0.27197	$n \rightarrow \pi^*$
			65→71	0.14545	
			69→71	0.10923	
			69→72	0.29602	
			70→72	0.45446	
			70→73	0.16131	
$S_0 \rightarrow S_{13}$	5.2144 eV/237.77 nm	0.0502	62→71	0.15481	$\pi \rightarrow \pi^*$
			63→71	0.63135	$n \rightarrow \pi^*$
			65→71	0.14702	

			67→72	0.10063	
			70→72	0.11268	
$S_0 \rightarrow S_{14}$	5.3371 eV/232.31 nm	0.4356	64→71	0.38475	$\pi \rightarrow \pi^*$
			69→71	0.10362	$n \rightarrow \pi^*$
			69→72	0.47110	
			70→72	0.10915	
			70→74	0.27718	
$S_0 \rightarrow S_{15}$	5.5085 eV/225.08 nm	0.0029	66→73	0.36378	$\pi \rightarrow \pi^*$
			67→73	0.11140	$n \rightarrow \pi^*$
			68→73	0.57699	
$S_0 \rightarrow S_{16}$	5.5752 eV/222.39 nm	0.0003	69→73	0.68212	$\pi \rightarrow \pi^*$
			70→73	0.12192	$n \rightarrow \pi^*$
$S_0 \rightarrow S_{17}$	5.7331 eV/216.26 nm	0.0001	63→71	0.13211	$\pi \rightarrow \pi^*$
			66→72	0.21190	$n \rightarrow \pi^*$
			67→72	0.62422	
			68→72	0.11553	
$S_0 \rightarrow S_{18}$	5.8122 eV/213.32 nm	0.0000	65→73	0.61830	$\pi \rightarrow \pi^*$
			66→73	0.22808	$n \rightarrow \pi^*$
			67→73	0.16972	
$S_0 \rightarrow S_{19}$	5.8768 eV/210.97 nm	0.0737	61→71	0.11352	$\pi \rightarrow \pi^*$
			69→72	0.23774	$n \rightarrow \pi^*$
			69→75	0.15478	
			70→74	0.60342	
$S_0 \rightarrow S_{20}$	6.0100 eV/206.30 nm	0.0043	66→72	0.23988	$\pi \rightarrow \pi^*$
			66→73	0.26573	$n \rightarrow \pi^*$
			67→73	0.50660	
			68→73	0.25529	
			68→74	0.17481	
$S_0 \rightarrow T_1$	2.5195 eV/492.10 nm	0.0000	69→71	0.27772	$\pi \rightarrow \pi^*$
			69→74	0.10571	$n \rightarrow \pi^*$
			70→71	0.61504	
			70→72	0.14177	
$S_0 \rightarrow T_2$	2.8511 eV/434.86 nm	0.0000	69→71	0.60825	$\pi \rightarrow \pi^*$
			70→71	0.31744	$n \rightarrow \pi^*$
$S_0 \rightarrow T_3$	2.9482 eV/420.54 nm	0.0000	67→71	0.19306	$\pi \rightarrow \pi^*$
			68→71	0.65887	$n \rightarrow \pi^*$
$S_0 \rightarrow T_4$	3.7501 eV/330.62 nm	0.0000	62→71	0.11074	$\pi \rightarrow \pi^*$
			63→71	0.16309	$n \rightarrow \pi^*$
			66→71	0.20360	
			67→71	0.57931	
			68→71	0.20044	
$S_0 \rightarrow T_5$	3.8512 eV/321.94 nm	0.0000	69→71	0.17336	$\pi \rightarrow \pi^*$
			70→72	0.63940	$n \rightarrow \pi^*$

[a] Oscillator strength. It is zero for $S_0 \rightarrow T_n$ transitions.
[b] Only the main configurations are presented.
[c] The CI coefficients are in absolute values.

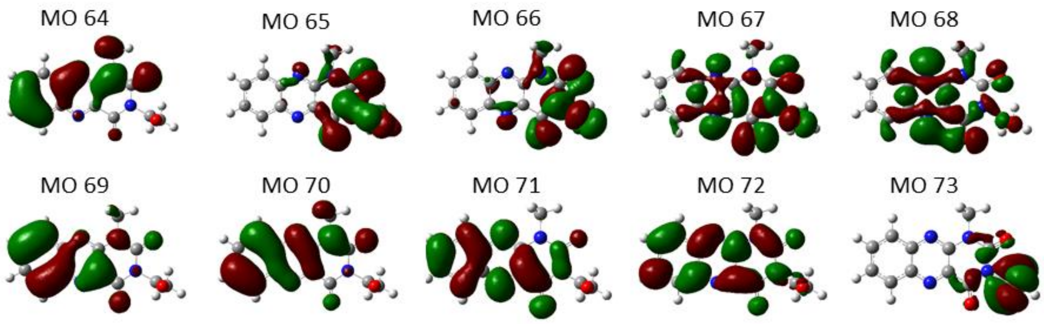

Figure S7. Contour plots of wavefunction of states of AAz3Me involved in absorption in visible light region. The C, O, N and H are in gray, red, blue and white, respectively. The isovalue is ±0.02 a.u.

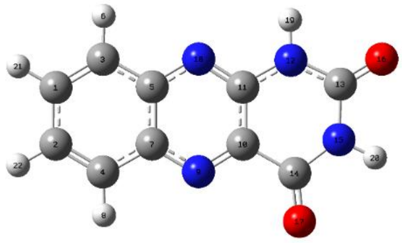

Figure S8. The optimized structure of S_0 of Az calculated at B3LYP/6-311g(d) level. The C, O, N and H are in gray, red, blue and white, respectively.

Table S8. Mulliken charge analysis of Az in S_0, S_1 and T_1.

Number[a]	Element	S_0	S_1	T_1	S_1-S_0[b]	T_1-S_0[c]
1	C	-0.1862	-0.1882	-0.1942	-0.0020	-0.0080
2	C	-0.1942	-0.1669	-0.1626	0.0274	0.0316
3	C	-0.1991	-0.1696	-0.1751	0.0294	0.0239
4	C	-0.1892	-0.1716	-0.2010	0.0176	-0.0119
5	C	0.1502	0.1451	0.1520	-0.0051	0.0018
6	H	0.2120	0.2313	0.2278	0.0193	0.0158
7	C	0.1363	0.1560	0.1614	0.0197	0.0251
8	H	0.2209	0.2402	0.2314	0.0193	0.0104
9	N	-0.2726	-0.3438	-0.3267	-0.0711	-0.0540
10	C	-0.1098	-0.1199	-0.1245	-0.0101	-0.0148
11	C	0.5142	0.5107	0.5147	-0.0035	0.0006
12	N	-0.6838	-0.6440	-0.6582	0.0398	0.0257
13	C	0.5838	0.5829	0.5770	-0.0009	-0.0068
14	C	0.4966	0.4623	0.4840	-0.0343	-0.0126
15	N	-0.6614	-0.6645	-0.6615	-0.0031	-0.0001
16	O	-0.3458	-0.3416	-0.3469	0.0042	-0.0012
17	O	-0.2980	-0.3325	-0.3192	-0.0345	-0.0212
18	N	-0.3413	-0.3785	-0.3637	-0.0372	-0.0225
19	H	0.3740	0.3758	0.3766	0.0018	0.0026
20	H	0.3757	0.3711	0.3723	-0.0047	-0.0034
21	H	0.2090	0.2189	0.2150	0.0099	0.0060
22	H	0.2085	0.2266	0.2215	0.0181	0.0130

[a] Numbers are consist with the optimized structure in Figure S8.
[b] The difference in Mulliken charges between S_1 and S_0.
[c] The difference in Mulliken charges between T_1 and S_0.

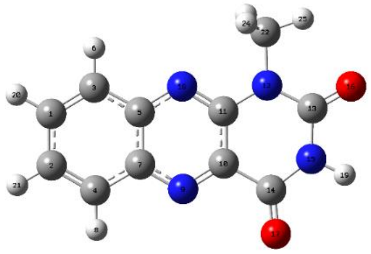

Figure S9. The optimized structure of S_0 of AzMe calculated at B3LYP/6-311g(d) level. The C, O, N and H are in gray, red, blue and white, respectively.

Table S9. Mulliken charge analysis of AzMe in S_0, S_1 and T_1.

Number[a]	Element	S_0	S_1	T_1	S_1-S_0[b]	T_1-S_0[c]
1	C	-0.1870	-0.1931	-0.1962	-0.0061	-0.0092
2	C	-0.1948	-0.1687	-0.1629	0.0261	0.0319
3	C	-0.1951	-0.1721	-0.1730	0.0230	0.0221
4	C	-0.1906	-0.1835	-0.2056	0.0071	-0.0150
5	C	0.1507	0.1419	0.1520	-0.0088	0.0013
6	H	0.2104	0.2230	0.2247	0.0126	0.0143
7	C	0.1308	0.1534	0.1588	0.0226	0.0280
8	H	0.2202	0.2334	0.2291	0.0133	0.0089
9	N	-0.2736	-0.3421	-0.3289	-0.0685	-0.0553
10	C	-0.0931	-0.1109	-0.1165	-0.0178	-0.0233
11	C	0.4853	0.4816	0.4886	-0.0037	0.0033
12	N	-0.4657	-0.4231	-0.4431	0.0426	0.0226
13	C	0.5793	0.5838	0.5748	0.0044	-0.0045
14	C	0.4985	0.4645	0.4849	-0.0340	-0.0135
15	N	-0.6606	-0.6623	-0.6582	-0.0018	0.0023
16	O	-0.3574	-0.3453	-0.3570	0.0121	0.0003
17	O	-0.3010	-0.3332	-0.3224	-0.0322	-0.0214
18	N	-0.3594	-0.3898	-0.3780	-0.0304	-0.0186
19	H	0.3743	0.3710	0.3711	-0.0033	-0.0032
20	H	0.2077	0.2135	0.2127	0.0057	0.0050
21	H	0.2075	0.2214	0.2197	0.0139	0.0122
22	C	-0.5110	-0.5141	-0.5118	-0.0031	-0.0007
23	H	0.2343	0.2440	0.2385	0.0097	0.0042
24	H	0.2343	0.2440	0.2385	0.0097	0.0041
25	H	0.2560	0.2627	0.2603	0.0067	0.0043

[a] Numbers are consist with the optimized structure of Figure S9.
[b] The difference of Mulliken charges between S_1 and S_0.
[c] The difference of Mulliken charges between T_1 and S_0.

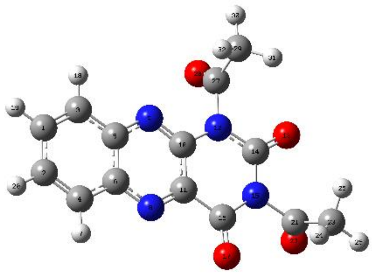

Figure S10. The optimized structure of S_0 of AAz13 calculated at B3LYP/6-311g(d) level. The C, O, N and H are in gray, red, blue and white, respectively.

Table S10. Mulliken charge analysis of AAz13 in S_0, S_1 and T_1.

Number[a]	Element	S_0	S_1	T_1	S_1-S_0[b]	T_1-S_0[c]
1	C	-0.1860	-0.1886	-0.1942	-0.0026	-0.0083
2	C	-0.1930	-0.1660	-0.1615	0.0270	0.0316
3	C	-0.1951	-0.1680	-0.1703	0.0271	0.0248
4	C	-0.1919	-0.1771	-0.2024	0.0148	-0.0105
5	C	0.1527	0.1497	0.1558	-0.0031	0.0031
6	C	0.1366	0.1560	0.1621	0.0195	0.0255
7	H	0.2224	0.2403	0.2334	0.0179	0.0110
8	N	-0.2724	-0.3423	-0.3261	-0.0700	-0.0538
9	N	-0.3645	-0.4031	-0.3875	-0.0387	-0.0231
10	C	0.5034	0.5008	0.5072	-0.0026	0.0038
11	C	-0.0716	-0.0807	-0.0916	-0.0090	-0.0200
12	N	-0.5221	-0.4825	-0.4979	0.0396	0.0242
13	O	-0.3691	-0.3486	-0.3661	0.0206	0.0030
14	C	0.5955	0.5963	0.5896	0.0008	-0.0059
15	N	-0.5000	-0.5050	-0.4981	-0.0050	0.0019
16	C	0.4773	0.4415	0.4640	-0.0358	-0.0133
17	O	-0.3104	-0.3474	-0.3352	-0.0370	-0.0249
18	H	0.2158	0.2338	0.2324	0.0179	0.0165
19	H	0.2108	0.2200	0.2173	0.0092	0.0064
20	H	0.2101	0.2273	0.2232	0.0172	0.0132
21	C	0.3842	0.3861	0.3854	0.0019	0.0012
22	O	-0.2272	-0.2389	-0.2326	-0.0117	-0.0054
23	C	-0.6758	-0.6783	-0.6765	-0.0025	-0.0007
24	H	0.2516	0.2636	0.2572	0.0121	0.0056
25	H	0.2463	0.2321	0.2389	-0.0142	-0.0074
26	H	0.2478	0.2415	0.2442	-0.0063	-0.0035
27	C	0.3818	0.3817	0.3808	-0.0001	-0.0011
28	O	-0.2265	-0.2204	-0.2238	0.0061	0.0027
29	C	-0.6749	-0.6742	-0.6736	0.0007	0.0013
30	H	0.2473	0.2481	0.2472	0.0007	-0.0001
31	H	0.2541	0.2564	0.2562	0.0023	0.0021
32	H	0.2429	0.2461	0.2430	0.0032	0.0001

[a] Numbers are consist with the optimized structure of Figure S10.
[b] The difference of Mulliken charges between S_1 and S_0.
[c] The difference of Mulliken charges between T_1 and S_0.

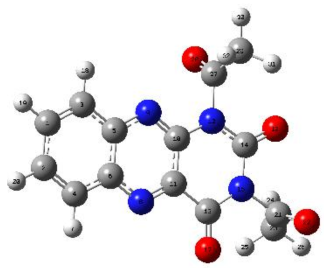

Figure S11. The optimized structure of S_0 of AAz13-1 calculated at B3LYP/6-311g(d) level. The C, O, N and H are in gray, red, blue and white, respectively.

Table S11. Mulliken charge analysis of AAz13 in S_0, S_1 and T_1.

Number[a]	**Element**	**S_0**	**S_1**	**T_1**	**S_1-S_0**[b]	**T_1-S_0**[c]
1	C	-0.1860	-0.1884	-0.1941	-0.0025	-0.0081
2	C	-0.1930	-0.1660	-0.1617	0.0270	0.0313
3	C	-0.1949	-0.1675	-0.1701	0.0274	0.0248
4	C	-0.1918	-0.1767	-0.2021	0.0151	-0.0103
5	C	0.1527	0.1495	0.1557	-0.0032	0.0030
6	C	0.1367	0.1558	0.1620	0.0191	0.0253
7	H	0.2223	0.2403	0.2334	0.0180	0.0110
8	N	-0.2725	-0.3428	-0.3261	-0.0703	-0.0536
9	N	-0.3636	-0.4025	-0.3866	-0.0389	-0.0229
10	C	0.5046	0.5022	0.5084	-0.0024	0.0038
11	C	-0.0719	-0.0805	-0.0918	-0.0086	-0.0199
12	N	-0.5225	-0.4833	-0.4985	0.0392	0.0240
13	O	-0.3700	-0.3493	-0.3674	0.0207	0.0026
14	C	0.5945	0.5953	0.5884	0.0008	-0.0060
15	N	-0.4994	-0.5043	-0.4974	-0.0050	0.0020
16	C	0.4767	0.4403	0.4634	-0.0363	-0.0132
17	O	-0.3105	-0.3479	-0.3352	-0.0373	-0.0246
18	H	0.2158	0.2338	0.2323	0.0180	0.0166
19	H	0.2108	0.2200	0.2172	0.0092	0.0065
20	H	0.2100	0.2273	0.2232	0.0173	0.0131
21	C	0.3826	0.3852	0.3841	0.0026	0.0016
22	O	-0.2313	-0.2432	-0.2367	-0.0119	-0.0054
23	C	-0.6757	-0.6773	-0.6763	-0.0016	-0.0005
24	H	0.2522	0.2378	0.2449	-0.0144	-0.0073
25	H	0.2528	0.2636	0.2577	0.0107	0.0048
26	H	0.2465	0.2403	0.2431	-0.0062	-0.0034
27	C	0.3801	0.3803	0.3793	0.0001	-0.0008
28	O	-0.2310	-0.2244	-0.2284	0.0066	0.0026
29	C	-0.6742	-0.6733	-0.6731	0.0009	0.0011
30	H	0.2460	0.2471	0.2461	0.0011	0.0001
31	H	0.2602	0.2621	0.2622	0.0019	0.0019
32	H	0.2440	0.2467	0.2439	0.0027	-0.0001

[a] Numbers are consist with the optimized structure of Figure S11.
[b] The difference of Mulliken charges between S_1 and S_0.
[c] The difference of Mulliken charges between T_1 and S_0.

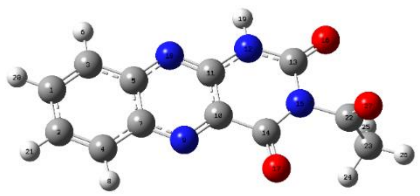

Figure S12. The optimized structure of S_0 of AAz3 calculated at B3LYP/6-311g(d) level. The C, O, N and H are in gray, red, blue and white, respectively.

Table S12. Mulliken charge analysis of AAz3 in S_0, S_1 and T_1.

Number[a]	Element	S_0	S_1	T_1	S_1-S_0[b]	T_1-S_0[c]
1	C	-0.1860	-0.1878	-0.1939	-0.0018	-0.0079
2	C	-0.1935	-0.1659	-0.1620	0.0276	0.0315
3	C	-0.1986	-0.1682	-0.1733	0.0304	0.0253
4	C	-0.1910	-0.1726	-0.2009	0.0184	-0.0100
5	C	0.1490	0.1437	0.1502	-0.0053	0.0012
6	H	0.2129	0.2332	0.2297	0.0203	0.0168
7	C	0.1411	0.1597	0.1658	0.0186	0.0247
8	H	0.2218	0.2414	0.2329	0.0196	0.0111
9	N	-0.2721	-0.3417	-0.3254	-0.0696	-0.0533
10	C	-0.0940	-0.1002	-0.1091	-0.0062	-0.0152
11	C	0.5240	0.5215	0.5266	-0.0025	0.0026
12	N	-0.6907	-0.6507	-0.6662	0.0400	0.0245
13	C	0.5896	0.5880	0.5816	-0.0017	-0.0080
14	C	0.4732	0.4357	0.4604	-0.0376	-0.0128
15	N	-0.4990	-0.5053	-0.4976	-0.0064	0.0014
16	O	-0.3555	-0.3364	-0.3532	0.0191	0.0023
17	O	-0.3115	-0.3499	-0.3362	-0.0384	-0.0247
18	N	-0.3401	-0.3738	-0.3619	-0.0337	-0.0218
19	H	0.3745	0.3769	0.3768	0.0024	0.0023
20	H	0.2099	0.2204	0.2166	0.0106	0.0067
21	H	0.2095	0.2281	0.2228	0.0187	0.0133
22	C	0.3876	0.3902	0.3890	0.0026	0.0014
23	C	-0.6759	-0.6785	-0.6763	-0.0027	-0.0005
24	H	0.2505	0.2631	0.2557	0.0126	0.0052
25	H	0.2493	0.2335	0.2417	-0.0158	-0.0076
26	H	0.2462	0.2396	0.2428	-0.0066	-0.0034
27	O	-0.2315	-0.2442	-0.2367	-0.0127	-0.0052

[a] Numbers are consist with the optimized structure of Figure S12.
[b] The difference of Mulliken charges between S_1 and S_0.
[c] The difference of Mulliken charges between T_1 and S_0.

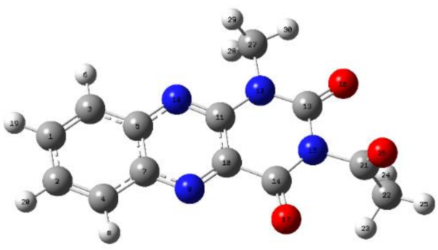

Figure S13. The optimized structure of S_0 of AAz3Me calculated at B3LYP/6-311g(d) level. The C, O, N and H are in gray, red, blue and white, respectively.

Table S13. Mulliken charge analysis of AAz3Me in S_0, S_1 and T_1.

Number[a]	Element	S_0	S_1	T_1	S_1-S_0[b]	T_1-S_0[c]
1	C	-0.1868	-0.1922	-0.1957	-0.0055	-0.0089
2	C	-0.1941	-0.1680	-0.1623	0.0262	0.0318
3	C	-0.1946	-0.1706	-0.1712	0.0241	0.0235
4	C	-0.1925	-0.1841	-0.2054	0.0084	-0.0129
5	C	0.1495	0.1409	0.1505	-0.0085	0.0010

6	H	0.2112	0.2250	0.2265	0.0137	0.0153
7	C	0.1360	0.1574	0.1633	0.0213	0.0272
8	H	0.2210	0.2349	0.2309	0.0138	0.0098
9	N	-0.2729	-0.3407	-0.3273	-0.0678	-0.0544
10	C	-0.0787	-0.0922	-0.1021	-0.0135	-0.0234
11	C	0.4947	0.4911	0.4994	-0.0036	0.0047
12	N	-0.4684	-0.4265	-0.4468	0.0419	0.0216
13	C	0.5828	0.5851	0.5763	0.0023	-0.0066
14	C	0.4762	0.4414	0.4639	-0.0347	-0.0123
15	N	-0.4951	-0.4981	-0.4902	-0.0031	0.0049
16	O	-0.3685	-0.3459	-0.3675	0.0226	0.0010
17	O	-0.3146	-0.3518	-0.3385	-0.0372	-0.0239
18	N	-0.3583	-0.3870	-0.3767	-0.0287	-0.0184
19	H	0.2087	0.2152	0.2143	0.0065	0.0057
20	H	0.2085	0.2230	0.2211	0.0145	0.0126
21	C	0.3863	0.3873	0.3868	0.0011	0.0005
22	C	-0.6755	-0.6765	-0.6759	-0.0010	-0.0004
23	H	0.2503	0.2621	0.2535	0.0118	0.0032
24	H	0.2482	0.2343	0.2427	-0.0139	-0.0055
25	H	0.2451	0.2402	0.2422	-0.0050	-0.0029
26	O	-0.2331	-0.2421	-0.2372	-0.0090	-0.0041
27	C	-0.5145	-0.5177	-0.5151	-0.0032	-0.0007
28	H	0.2343	0.2435	0.2376	0.0092	0.0034
29	H	0.2373	0.2465	0.2409	0.0092	0.0037
30	H	0.2575	0.2655	0.2620	0.0080	0.0045

[a] Numbers are consist with the optimized structure of Figure S13.
[b] The difference of Mulliken charges between S_1 and S_0.
[c] The difference of Mulliken charges between T_1 and S_0.

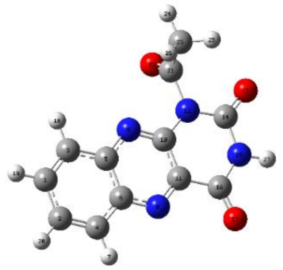

Figure S14. The optimized structure of S_0 of AAz1 calculated at B3LYP/6-311g(d) level. The C, O, N and H are in gray, red, blue and white, respectively.

Table S14. Mulliken charge analysis of AAz1 in S_0, S_1 and T_1.

Number[a]	Element	S_0	S_1	T_1	S_1-S_0[b]	T_1-S_0[c]
1	C	-0.1862	-0.1890	-0.1945	-0.0028	-0.0083
2	C	-0.1935	-0.1668	-0.1622	0.0268	0.0314
3	C	-0.1954	-0.1689	-0.1717	0.0264	0.0237
4	C	-0.1898	-0.1756	-0.2017	0.0142	-0.0118
5	C	0.1540	0.1511	0.1575	-0.0029	0.0035
6	C	0.1317	0.1521	0.1577	0.0204	0.0259
7	H	0.2217	0.2393	0.2322	0.0176	0.0105
8	N	-0.2729	-0.3444	-0.3270	-0.0716	-0.0541

9	N	-0.3651	-0.4070	-0.3885	-0.0419	-0.0234
10	C	0.4945	0.4920	0.4966	-0.0025	0.0021
11	C	-0.0870	-0.0997	-0.1070	-0.0126	-0.0200
12	N	-0.5186	-0.4787	-0.4936	0.0399	0.0250
13	O	-0.3581	-0.3504	-0.3592	0.0077	-0.0012
14	C	0.5913	0.5926	0.5859	0.0012	-0.0054
15	N	-0.6654	-0.6676	-0.6643	-0.0022	0.0011
16	C	0.5000	0.4661	0.4868	-0.0339	-0.0132
17	O	-0.2954	-0.3289	-0.3173	-0.0335	-0.0218
18	H	0.2151	0.2323	0.2310	0.0171	0.0159
19	H	0.2100	0.2186	0.2160	0.0086	0.0060
20	H	0.2093	0.2261	0.2221	0.0168	0.0128
21	C	0.3849	0.3846	0.3839	-0.0003	-0.0009
22	O	-0.2311	-0.2249	-0.2282	0.0062	0.0029
23	C	-0.6746	-0.6738	-0.6735	0.0008	0.0011
24	H	0.2458	0.2465	0.2459	0.0008	0.0001
25	H	0.2563	0.2564	0.2575	0.0001	0.0012
26	H	0.2425	0.2466	0.2431	0.0041	0.0007
27	H	0.3759	0.3714	0.3723	-0.0044	-0.0035

[a] Numbers are consist with the optimized structure of Figure S14.
[b] The difference of Mulliken charges between S_1 and S_0.
[c] The difference of Mulliken charges between T_1 and S_0.

Table S15. The contribution of vibrational normal modes to reorganization energy for $S_1 \rightarrow S_0$ transition of AZs.

	E_{reorg}(tol)/cm^{-1}	Mode	Freq/cm^{-1}	E_{reorg}/cm^{-1}
Az	2187.52	11	197.25	157.88
		16	416.36	59.06
		24	618.44	347.41
		43	1173.71	54.45
		44	1241.18	205.73
		46	1277.65	146.92
		49	1382.99	75.07
		53	1467.04	73.71
		56	1598.96	506.54
		57	1611.11	118.82
		58	1662.09	112.31
AAz1	2197.18	15	220.18	130.55
		30	622.23	341.63
		53	1185.78	55.82
		54	1244.52	229.34
		56	1281.47	114.27
		61	1401.45	55.49
		63	1458.25	51.80
		69	1598.20	557.33
		70	1659.17	129.96
		72	1780.40	52.19
		73	1862.58	7.31
		74	3052.43	1.50
AAz3	4804.81	7	27.12	65.79
		15	213.62	108.53
		17	261.85	53.98
		29	591.19	79.25
		31	618.38	635.10
		32	668.28	205.96
		42	913.24	56.77
		43	939.10	60.16
		45	1002.65	489.59
		54	1241.62	279.35
		56	1276.48	126.36
		59	1383.65	62.32
		63	1459.63	132.57
		68	1597.41	433.61
		69	1611.55	161.57
		70	1662.24	107.88
		71	1731.54	75.43
		72	1772.57	75.14
		73	1864.22	789.02
		74	3052.43	230.81
AAz13	4338.99	8	28.76	57.07
		19	233.42	84.54
		36	605.48	180.99

		37	617.21	537.75
		42	763.11	134.35
		50	961.84	86.44
		52	1000.80	296.84
		53	1011.05	108.96
		62	1186.90	52.12
		64	1245.07	301.49
		66	1280.98	100.68
		73	1451.09	112.95
		80	1590.08	81.49
		81	1598.75	505.73
		82	1658.89	121.48
		84	1761.12	112.41
		85	1862.80	199.58
		86	1870.01	418.44
		87	3052.27	215.78
AAz13-1	3954.89	19	233.67	84.81
		36	605.71	64.63
		37	619.07	559.42
		42	762.77	134.32
		50	961.26	77.38
		52	1000.84	239.22
		53	1011.28	69.64
		62	1186.88	51.34
		64	1245.34	302.01
		66	1280.99	99.78
		73	1450.86	110.19
		80	1589.97	83.28
		81	1598.74	512.44
		82	1658.88	120.49
		84	1761.19	107.74
		85	1862.58	123.3
		86	1867.79	379.14
		88	3052.66	173.27
AzMe	2032.19	12	187.69	112.20
		19	408.50	59.96
		26	621.75	264.33
		47	1184.77	86.34
		49	1259.65	103.15
		51	1296.54	205.07
		53	1385.92	76.37
		55	1403.67	80.87
		64	1599.52	496.58
		65	1658.97	117.75
AAz3Me	3160.394	7	36.14	70.92
		16	201.09	90.66
		32	604.16	68.26

	33	617.04	414.41
	43	862.84	102.40
	47	998.95	81.41
	48	1003.82	142.77
	58	1232.80	78.95
	59	1258.43	154.56
	61	1294.15	213.17
	64	1387.07	76.10
	76	1599.25	472.90
	77	1658.98	109.07
	79	1759.46	67.13
	80	1863.49	282.65
	81	3052.89	99.20

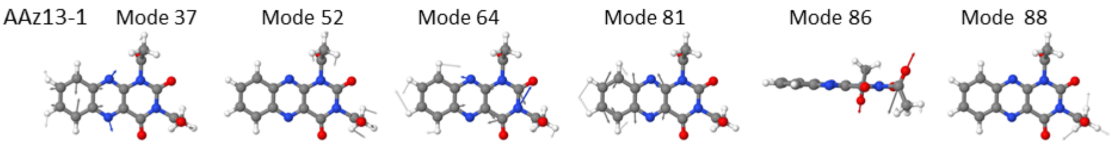

Figure S15. The E_{reorg} vectorized representation of atomic displacement for the corresponding vibration normal modes of AAz13-1 $S_1 \rightarrow S_0$ transition.

Table S16. The contribution of vibrational normal modes to Huang-Rhys factors for $S_1 \rightarrow S_0$ transitions of AZs.

	HR(tol)	Mode	Freq/cm^{-1}	HR
Az	2.7006	11	200.14	0.8002
		22	585.53	0.4225
		16	416.11	0.1413
		24	576.00	0.1686
		26	663.99	0.0773
		44	1194.44	0.1319
		48	1344.67	0.1291
		51	1422.27	0.0601
		53	1438.01	0.0780
		56	1492.71	0.1535
		57	1526.72	0.1044
		59	1705.62	0.1014
AAz1	3.1307	7	46.09	0.1927
		9	69.13	0.0980
		11	118.01	0.2410
		15	215.66	0.5879
		28	572.20	0.1844
		29	617.10	0.1147
		30	580.05	0.2028
		32	646.70	0.1488
		54	1194.89	0.1153
		62	1408.81	0.0994
		69	1486.86	0.2560
		72	1710.58	0.0915
AAz3	9.4948	7	50.07	2.4406
		8	41.16	1.5537
		9	71.57	0.3956
		15	228.44	0.8339
		22	434.10	0.1533
		26	546.17	0.1750
		28	566.81	0.3964
		31	580.17	0.1899
		32	683.03	0.1759
		33	662.36	0.3015
		43	941.26	0.1043
		45	988.70	0.4737
		53	1187.39	0.1440
		63	1433.51	0.1305
		68	1492.10	0.1591
		71	1675.79	0.1501
		73	1844.09	0.5386
AAz13	8.4153	7	45.10	1.1671
		8	33.87	1.4788
		9	49.86	0.4996
		11	76.61	0.5458
		13	116.58	0.2421

		19	242.96	0.7001
		27	434.78	0.1180
		34	560.57	0.3426
		37	579.30	0.1776
		38	631.95	0.4721
		50	959.88	0.1657
		52	995.38	0.3616
		63	1187.42	0.1122
		81	1487.09	0.1770
		83	1676.89	0.1223
		85	1847.04	0.4088
AAz13-1	7.4815	7	33.47	1.9583
		8	48.84	0.6023
		10	57.9	0.4920
		13	116.81	0.2315
		19	241.78	0.6469
		34	560.99	0.3603
		37	579.66	0.1204
		38	630.01	0.3704
		50	959.02	0.1461
		52	996.78	0.1187
		53	996.14	0.2187
		63	1187.52	0.1108
		81	1487.9	0.2102
		83	1676.62	0.1184
		86	1846.92	0.3420
AzMe	2.4047	12	189.86	0.6035
		15	317.99	0.0973
		19	410.64	0.1480
		25	611.87	0.1164
		26	576.55	0.2678
		28	658.82	0.0989
		51	1201.21	0.1427
		54	1396.32	0.1535
		58	1449.36	0.1027
		64	1487.95	0.1181
		67	1707.96	0.0977
AAz3Me	5.4036	7	31.18	1.4086
		8	40.83	0.4757
		16	209.33	0.5983
		20	321.87	0.1527
		31	554.97	0.3058
		34	636.16	0.3769
		48	1005.78	0.2952
		61	1199.41	0.0998
		70	1449.53	0.0951
		78	1676.07	0.1195

		80	1848.99	0.2182

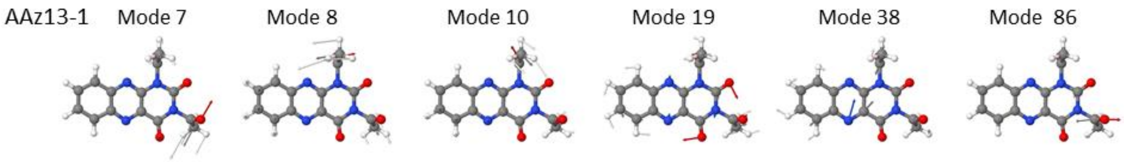

Figure S16. Decomposition of calculated Huang-Rhys factors (HRs) to vibrational normal modes of AAz13-1 for $S_1 \rightarrow S_0$ transition.

Table S17. Bond Length (Å) and Dihedral Angle (°) of Az calculated at B3LYP/6-311g(d) level.

	S_0	S_1	$S_1 \rightarrow S_0$
L(N1-C10a)	1.38	1.36	-0.02
L(N1-C2)	1.38	1.40	0.02
L(C2-N3)	1.39	1.37	-0.02
L(N3-C4)	1.39	1.42	0.03
D(H-N1-C10a-C4a)	-179.97	179.99	—
D(H-N1-C2-N3)	179.98	-179.98	—
D(C4a-C10a-N1-C2)	0.01	-0.01	0.01
D(C10a)N1-C2-N3)	-0.01	0.02	-0.01
D(H-N3-C4-C4a)	180.00	-179.99	—
D(H-N3-C2-N1)	-179.99	179.98	—
D(N1-C2-N3-C4)	0.00	-0.02	0.00
D(C4a-C4-N3-C2)	0.01	0.01	0.01

Table S18. Bond Length (Å) and Dihedral Angle (°) of AAz1 calculated at B3LYP/6-311g(d) level.

	S_0	S_1	$S_1 \rightarrow S_0$
L(N1-C10a)	1.39	1.37	-0.02
L(N1-C2)	1.38	1.41	0.03
L(C2-N3)	1.39	1.36	-0.03
L(N3-C4)	1.39	1.42	0.03
D(C-N1-C10a-C4a)	176.03	175.86	-0.17
D(C-N1-C2-N3)	-176.60	-176.39	0.21
D(O-C-N1-C10a)	-82.64	-89.26	-6.62
D(O-C-N1-C2)	95.14	88.60	-6.54
D(C4a-C10a-N1-C2)	-1.58	-1.82	-0.24
D(C10a)N1-C2-N3)	1.07	1.36	0.29
D(H-N3-C4-C4a)	179.70	179.34	-0.37
D(H-N3-C2-N1)	179.53	-179.97	
D(N1-C2-N3-C4)	0.42	-0.18	-0.59
D(C4a-C4-N3-C2)	-1.20	-0.46	0.73

Table S19. Bond Length (Å) and Dihedral Angle (°) of AAz3 calculated at B3LYP/6-311g(d) level.

	S_0	S_1	$S_1 \rightarrow S_0$
L(N1-C10a)	1.38	1.36	-0.02
L(N1-C2)	1.38	1.40	0.02
L(C2-N3)	1.40	1.38	-0.02
L(N3-C4)	1.40	1.44	0.04
D(H-N1-C10a-C4a)	179.37	179.43	0.06
D(H-N1-C2-N3)	179.69	-179.56	—
D(C4a-C10a-N1-C2)	-0.46	1.02	1.48
D(C10a-N1-C2-N3)	-0.48	-1.16	-0.68
D(C-N3-C4-C4a)	177.05	178.41	1.36
D(C-N3-C2-N1)	-177.21	-177.07	0.14
D(O-C-N3-C2)	91.08	66.60	-24.48
D(O-C-N3-C4)	-88.06	-110.53	-22.47
D(N1-C2-N3-C4)	1.83	-0.24	-2.06
D(C4a-C4-N3-C2)	-1.97	1.58	3.56

Table S20. Bond Length (Å) and Dihedral Angle (°) of AAz13 calculated at B3LYP/6-311g(d) level.

	S_0	S_1	$S_1 \rightarrow S_0$
L(N1-C10a)	1.39	1.37	-0.02
L(N1-C2)	1.38	1.41	0.03
L(C2-N3)	1.39	1.37	-0.02
L(N3-C4)	1.40	1.44	0.04
D(C-N1-C10a-C4a)	176.81	176.28	-0.53
D(C-N1-C2-N3)	-176.30	-176.36	-0.06
D(O-C-N1-C10a)	-83.67	-90.34	-6.67
D(O-C-N1-C2)	94.31	88.45	-5.86
D(C4a-C10a-N1-C2)	-1.03	-2.41	-1.38
D(C10a-N1-C2-N3)	1.58	2.36	0.78
D(C-N3-C4-C4a)	-177.29	-179.08	-1.79
D(C-N3-C2-N1)	176.61	176.98	0.37
D(O-C-N3-C2)	-89.19	-67.72	21.47
D(O-C-N3-C4)	89.16	109.51	20.35
D(N1-C2-N3-C4)	-1.54	0.04	1.58
D(C4a-C4-N3-C2)	0.85	-2.14	-2.99

Table S21. Bond Length (Å) and Dihedral Angle (°) of AAz13-1 calculated at B3LYP/6-311g(d) level.

	S_0	S_1	$S_1 \rightarrow S_0$
L(N1-C10a)	1.39	1.37	-0.02
L(N1-C2)	1.38	1.41	0.03
L(C2-N3)	1.39	1.37	-0.02
L(N3-C4)	1.40	1.44	0.04
D(C-N1-C10a-C4a)	174.92	174.97	0.05
D(C-N1-C2-N3)	-176.37	-175.68	0.69
D(O-C-N1-C10a)	-80.89	-87.10	-6.21
D(O-C-N1-C2)	95.92	89.36	-6.56
D(C4a-C10a-N1-C2)	-1.66	-1.17	0.49
D(C10a-N1-C2-N3)	-1.66	-1.17	0.49
D(C-N3-C4-C4a)	176.69	177.17	0.48
D(C-N3-C2-N1)	-177.31	-176.91	0.40
D(O-C-N3-C2)	89.49	68.45	-21.03
D(O-C-N3-C4)	-89.96	-108.50	-18.54
D(N1-C2-N3-C4)	2.08	-0.27	-2.34
D(C4a-C4-N3-C2)	-2.69	0.53	3.22

Table S22. Bond Length (Å) and Dihedral Angle (°) of AzMe calculated at B3LYP/6-311g(d) level.

	S_0	S_1	$S_1 \rightarrow S_0$
L(N1-C10a)	1.39	1.37	-0.01
L(N1-C2)	1.39	1.42	0.04
L(C2-N3)	1.39	1.36	-0.03
L(N3-C4)	1.39	1.42	0.03
D(C-N1-C10a-C4a)	179.96	-179.99	—
D(C-N1-C2-N3)	-180.00	179.99	—
D(C4a-C10a-N1-C2)	-0.03	0.02	0.05
D(C10a)N1-C2-N3)	0.00	-0.01	-0.01
D(H-N3-C4-C4a)	-180.00	-179.98	—
D(H-N3-C2-N1)	-179.98	180.00	—
D(N1-C2-N3-C4)	0.02	-0.01	-0.03
D(C4a-C4-N3-C2)	0.00	0.03	0.02

Table S23. Bond Length (Å) and Dihedral Angle (°) of AAz3Me calculated at B3LYP/6-311g(d) level.

	S_0	S_1	$S_1 \rightarrow S_0$
L(N1-C10a)	1.39	1.37	-0.02
L(N1-C2)	1.38	1.42	0.04
L(C2-N3)	1.40	1.37	-0.03
L(N3-C4)	1.39	1.43	0.04
D(C-N1-C10a-C4a)	179.37	179.71	0.34
D(C-N1-C2-N3)	179.54	179.49	-0.05
D(C4a-C10a-N1-C2)	-0.44	0.77	1.20
D(C10a)N1-C2-N3)	-0.65	-1.54	-0.89
D(C-N3-C4-C4a)	177.10	177.81	0.72
D(C-N3-C2-N1)	-177.15	-176.59	0.57
D(O-C-N3-C2)	91.53	72.72	-18.81
D(O-C-N3-C4)	-87.82	-105.19	-17.37
D(N1-C2-N3-C4)	2.11	1.07	-1.04
D(C4a-C4-N3-C2)	-2.16	0.15	2.31

Table S24. The contribution of vibrational normal mode to reorganization energy for $T_1 \rightarrow S_0$ transition of AZs.

	E_{reorg}(tol)/cm^{-1}	Mode	Freq/cm^{-1}	E_{reorg}/cm^{-1}
Az	3281.16	11	197.25	159.71
		16	416.36	63.92
		24	618.44	281.81
		43	1173.71	60.48
		44	1241.18	154.69
		49	1382.99	536.26
		50	1402.71	57.46
		52	1455.56	79.69
		53	1467.04	161.12
		56	1598.96	671.77
		57	1611.11	685.48
AAz1	3281.49	15	220.18	113.08
		30	622.23	276.19
		53	1185.78	70.24
		54	1244.52	133.68
		55	1274	57.25
		58	1379.66	204.32
		59	1385.77	287.99
		61	1401.45	121.22
		62	1439.43	75.09
		63	1458.25	194.27
		67	1532.37	76.47
		69	1598.2	1301.73
		70	1659.17	84.11
AAz3	3352.83	15	213.62	127.54
		28	565.14	67.34
		31	618.38	295.33
		52	1172.71	50.47
		54	1241.62	179.17
		59	1383.65	530.46
		63	1459.63	268.31
		68	1597.41	595.14
		69	1611.55	765
AAz13	3357.15	19	233.42	91.99
		34	564.68	54.73
		37	617.21	286.59
		62	1186.9	60.57
		64	1245.07	166.38
		68	1381.74	269.77
		69	1385.18	208.75
		73	1451.09	303.44
		79	1533.17	58.71
		81	1598.75	1314.67
		82	1658.89	78.3
AAz13-1	3329.35	19	233.67	89.96
		34	566.84	73.01

		37	619.07	267
		62	1186.88	60.56
		64	1245.34	165.85
		68	1381.47	241.08
		69	1385.07	235.81
		72	1401.64	53.53
		73	1450.86	303.86
		79	1533.13	57.69
		81	1598.74	1319.65
		82	1658.88	77.37
AzMe	3131.53	12	187.69	110.87
		19	408.5	56.89
		26	621.75	262.66
		47	1184.77	116.03
		49	1259.65	71.36
		50	1274.3	62.02
		53	1385.92	365.25
		54	1387.17	132.99
		55	1403.67	169.75
		56	1438.37	111.84
		58	1484.85	112.26
		63	1591.51	285.31
		64	1599.52	875.11
		65	1658.97	93.15
AAz3Me	3158.35	16	201.09	87.74
		31	564	65.05
		33	617.04	194.82
		58	1232.8	56.18
		59	1258.43	105.99
		63	1386.08	183.03
		64	1387.07	328.34
		66	1406.44	89.38
		67	1438.94	142.44
		70	1481.35	107.68
		75	1589.67	87.02
		76	1599.25	1108.31
		77	1658.98	86.43

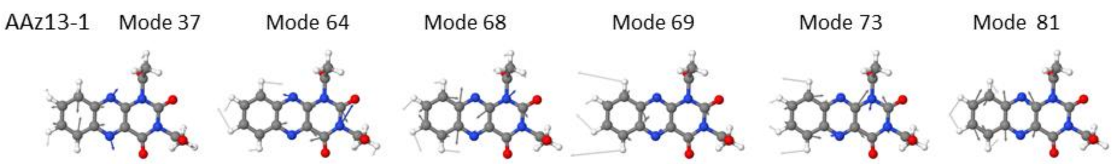

Figure S17. The E_{reorg} vectorized representation of atomic displacement for the corresponding vibration normal modes of AAz13-1 $T_1 \rightarrow S_0$ transition.

Table S25. The contribution of vibrational normal modes of Huang-Rhys factors for T_1-S_0 transition of AZs.

	HR(tol)	Mode	Freq/cm^{-1}	HR
Az	3.2467	11	193.33	0.7656
		14	329.64	0.0712
		16	417.54	0.1530
		24	594.67	0.4881
		43	1192.72	0.0950
		47	1279.61	0.0527
		48	1304.34	0.3341
		49	1380.47	0.1547
		53	1488.96	0.1444
		56	1580.80	0.3669
		57	1359.35	0.2260
AAz1	3.3473	7	37.36	0.0532
		11	117.28	0.3174
		15	210.93	0.4226
		19	328.78	0.0668
		26	522.99	0.0514
		29	591.54	0.2599
		30	609.64	0.1974
		39	780.15	0.0537
		53	1196.49	0.0750
		54	1226.87	0.0585
		57	1293.36	0.0617
		59	1341.65	0.1021
		63	1367.29	0.6737
		67	1522.19	0.0744
		69	1581.23	0.3621
AAz3	3.6190	7	19.80	0.3075
		11	129.56	0.1757
		15	210.15	0.5441
		19	333.30	0.0776
		22	439.52	0.0687
		28	552.18	0.1733
		29	584.29	0.1119
		31	597.37	0.2793
		53	1185.19	0.0923
		56	1307.68	0.3574
		58	1355.11	0.1535
		61	1377.35	0.2070
		63	1484.67	0.1364
		69	1585.41	0.3720
		71	1698.38	0.0514
AAz13	3.7539	7	38.12	0.1038
		8	14.81	0.2298
		13	115.14	0.3481
		19	229.99	0.3832
		24	335.96	0.0867

		34	553.34	0.1426
		36	602.31	0.1052
		37	592.19	0.1949
		38	626.98	0.0929
		67	1294.57	0.0516
		69	1338.49	0.1238
		73	1365.61	0.6300
		79	1521.94	0.0631
		80	1192.47	0.0972
		81	1584.00	0.3657
AAz13-1	3.7526	7	24.93	0.3354
		13	115.78	0.3165
		19	230.15	0.3466
		34	553.98	0.1447
		36	590.17	0.1957
		37	604.45	0.1017
		69	1338.55	0.1216
		73	1365.31	0.6359
		81	1584.56	0.3688
AzMe	2.9922	12	184.09	0.5626
		15	316.46	0.1454
		19	413.57	0.1422
		23	510.37	0.0535
		25	585.49	0.1297
		26	606.84	0.2863
		40	954.10	0.0534
		47	1188.27	0.1285
		49	1236.29	0.0847
		54	1348.41	0.1264
		58	1499.08	0.0551
		63	1368.45	0.5586
		64	1572.96	0.2862
AAz3Me	3.1417	7	33.39	0.1030
		13	129.35	0.1331
		16	197.08	0.3925
		20	316.93	0.1302
		24	435.14	0.0543
		31	553.60	0.1385
		32	584.16	0.1334
		33	603.17	0.1844
		56	1179.92	0.1293
		58	1242.98	0.0994
		63	1343.42	0.1395
		70	1494.48	0.0579
		75	1367.50	0.5394
		76	1578.05	0.3072

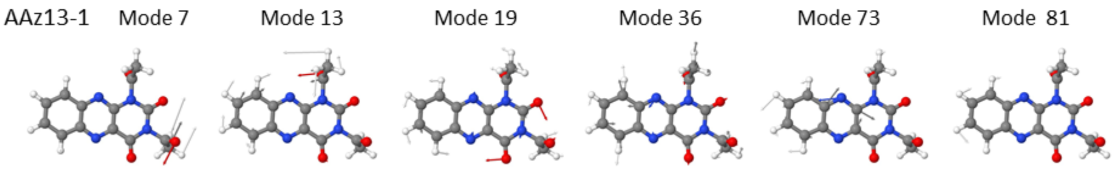

Figure S18. Decomposition of calculated Huang-Rhys factors (HRs) to vibrational normal modes of AAz13-1 for $T_1 \rightarrow S_0$ transition.

Table S26. The H_{SO} of AZs.

H_{SO}/cm^{-1}	$S_1 \rightarrow T_3$	$S_1 \rightarrow T_2$	$S_1 \rightarrow T_1$	$T_3 \rightarrow S_0$	$T_2 \rightarrow S_0$	$T_1 \rightarrow S_0$
Az	9.53	1.24×10^{-1}	1.55×10^{-1}	1.04×10^{-1}	8.52	1.71×10^{-1}
AzMe	8.63	1.44×10^{-1}	1.95×10^{-1}	1.35×10^{-1}	8.10	2.13×10^{-1}
AAz13	8.57	1.72×10^{-1}	3.40×10^{-1}	9.18×10^{-1}	7.83	2.82×10^{-1}
AAz13-1	8.53	3.03×10^{-1}	1.38×10^{-1}	1.03	7.75	5.14×10^{-1}
AAz3	9.11	9.93×10^{-2}	2.44×10^{-1}	2.79×10^{-1}	8.34	2.28×10^{-1}
AAz3Me	8.27	9.87×10^{-2}	2.49×10^{-1}	7.85×10^{-1}	7.90	2.65×10^{-1}
AAz1	8.78	2.00×10^{-1}	1.89×10^{-1}	1.10	7.87	4.16×10^{-1}

References:

1. A. D. Becke, *J. Chem. Phys.*, 1993, **98**, 5648-5652.
2. C. T. Lee, W. T. Yang and R. G. Parr, *Phys. Rev. B*, 1988, **37**, 785-789.
3. R. C. Binning and L. A. Curtiss, *J. Comput. Chem.*, 1990, **11**, 1206-1216.
4. M. M. Francl, W. J. Pietro, W. J. Hehre, J. S. Binkley, M. S. Gordon, D. J. Defrees and J. A. Pople, *J. Chem. Phys.*, 1982, **77**, 3654-3665.
5. V. A. Rassolov, M. A. Ratner, J. A. Pople, P. C. Redfern and L. A. Curtiss, *J. Comput. Chem.*, 2001, **22**, 976-984.
6. F. Weigend and R. Ahlrichs, *Phys. Chem. Chem. Phys.*, 2005, **7**, 3297-3305.
7. F. Weigend, *Phys. Chem. Chem. Phys.*, 2006, **8**, 1057-1065.
8. M. J. Frisch, G. W. Trucks, H. B. Schlegel, G. E. Scuseria, M. A. Robb, J. R. Cheeseman, G. Scalmani, V. Barone, G. A. Petersson, H. Nakatsuji, X. Li, M. Caricato, A. V. Marenich, J. Bloino, B. G. Janesko, R. Gomperts, B. Mennucci, H. P. Hratchian, J. V. Ortiz, A. F. Izmaylov, J. L. Sonnenberg, Williams, F. Ding, F. Lipparini, F. Egidi, J. Goings, B. Peng, A. Petrone, T. Henderson, D. Ranasinghe, V. G. Zakrzewski, J. Gao, N. Rega, G. Zheng, W. Liang, M. Hada, M. Ehara, K. Toyota, R. Fukuda, J. Hasegawa, M. Ishida, T. Nakajima, Y. Honda, O. Kitao, H. Nakai, T. Vreven, K. Throssell, J. A. Montgomery Jr., J. E. Peralta, F. Ogliaro, M. J. Bearpark, J. J. Heyd, E. N. Brothers, K. N. Kudin, V. N. Staroverov, T. A. Keith, R. Kobayashi, J. Normand, K. Raghavachari, A. P. Rendell, J. C. Burant, S. S. Iyengar, J. Tomasi, M. Cossi, J. M. Millam, M. Klene, C. Adamo, R. Cammi, J. W. Ochterski, R. L. Martin, K. Morokuma, O. Farkas, J. B. Foresman and D. J. Fox, *Gaussian 16 A 01*, 2016.
9. O. Vahtras, H. Agren, P. Jorgensen, H. J. A. Jensen, T. Helgaker and J. Olsen, *J. Chem. Phys.*, 1992, **97**, 9178-9187.
10. H. Hettema, H. J. A. Jensen, P. Jorgensen and J. Olsen, *J. Chem. Phys.*, 1992, **97**, 1174-1190.
11. H. Agren, O. Vahtras, H. Koch, P. Jorgensen and T. Helgaker, *J. Chem. Phys.*, 1993, **98**, 6417-6423.
12. J. Olsen, D. L. Yeager and P. Jorgensen, *J. Chem. Phys.*, 1989, **91**, 381-388.
13. P. Jorgensen, H. J. A. Jensen and J. Olsen, *J. Chem. Phys.*, 1988, **89**, 3654-3661.
14. K. Aidas, C. Angeli, K. L. Bak, V. Bakken, R. Bast, L. Boman, O. Christiansen, R. Cimiraglia, S. Coriani, P. Dahle, E. K. Dalskov, U. Ekstrom, T. Enevoldsen, J. J. Eriksen, P. Ettenhuber, B. Fernandez, L. Ferrighi, H. Fliegl, L. Frediani, K. Hald, A. Halkier, C. Hattig, H. Heiberg, T. Helgaker, A. C. Hennum, H. Hettema, E. Hjertenaes, S. Host, I. M. Hoyvik, M. F. Iozzi, B. Jansik, H. J. A. Jensen, D. Jonsson, P. Jorgensen, J. Kauczor, S. Kirpekar, T. Kjrgaard, W. Klopper, S. Knecht, R. Kobayashi, H. Koch, J. Kongsted, A. Krapp, K. Kristensen, A. Ligabue, O. B. Lutnaes, J. I. Melo, K. V. Mikkelsen, R. H. Myhre, C. Neiss, C. B. Nielsen, P. Norman, J. Olsen, J. M. H. Olsen, A. Osted, M. J. Packer, F. Pawlowski, T. B. Pedersen, P. F. Provasi, S. Reine, Z. Rinkevicius, T. A. Ruden, K. Ruud, V. V. Rybkin, P. Salek, C. C. M. Samson, A. S. de Meras, T. Saue, S. P. A. Sauer, B. Schimmelpfennig, K. Sneskov, A. H. Steindal, K. O. Sylvester-Hvid, P. R. Taylor, A. M. Teale, E. I. Tellgren, D. P. Tew, A. J. Thorvaldsen, L. Thogersen, O. Vahtras, M. A. Watson, D. J. D. Wilson, M. Ziolkowski and H. Agren, *Wiley Interdiscip. Rev.-Comput. Mol. Sci.*, 2014, **4**, 269-284.
15. Q. Peng, Y. P. Yi, Z. G. Shuai and J. S. Shao, *J. Chem. Phys.*, 2007, **126**, 114302.
16. Q. Peng, Y. P. Yi, Z. G. Shuai and J. S. Shao, *J. Am. Chem. Soc.*, 2007, **129**, 9333-9339.
17. Y. L. Niu, Q. A. Peng, C. M. Deng, X. Gao and Z. G. Shuai, *J. Phys. Chem. A*, 2010, **114**,

7817-7831.
18. Y. Niu, Q. Peng and Z. Shuai, *Sci. China Ser. B-Chem.*, 2008, **51**, 1153-1158.
19. Q. Peng, Y. L. Niu, Q. H. Shi, X. Gao and Z. G. Shuai, *J. Chem. Theory Comput.*, 2013, **9**, 1132-1143.
20. Z. G. Shuai, *Chin. J. Chem.*, 2020, **38**, 1223-1232.
21. Y. L. Niu, W. Q. Li, Q. Peng, H. Geng, Y. P. Yi, L. J. Wang, G. J. Nan, D. Wang and Z. G. Shuai, *Mol. Phys.*, 2018, **116**, 1078-1090.
22. Z. G. Shuai and Q. Peng, *Phys. Rep.-Rev. Sec. Phys. Lett.*, 2014, **537**, 123-156.
23. Z. G. Shuai and Q. Peng, *Natl. Sci. Rev.*, 2017, **4**, 224-239.
24. Y. Niu, Q. Peng, C. Deng, X. Gao and Z. Shuai, *J. Phys. Chem. A*, 2010, **114**, 7817-7831.
25. T. Lu and F. W. Chen, *J. Comput. Chem.*, 2012, **33**, 580-592.
26. S. Miertus, E. Scrocco and J. Tomasi, *Chem. Phys.*, 1981, **55**, 117-129.
27. R. Cammi and B. Mennucci, *J. Chem. Phys.*, 1999, **110**, 9877-9886.
28. J. Tomasi, B. Mennucci and R. Cammi, *Chem. Rev.*, 2005, **105**, 2999-3093.